Available online at www.sciencedirect.com
ScienceDirect
Developmental Biology 302 (2007) 477–493
DEVELOPMENTAL BIOLOGY
www.elsevier.com/locate/ydbio

PP2A:B56ε is required for eye induction and eye field separation

Anna M. Rorick [a], Wenyan Mei [a], Nicole L. Liette [a], Christopher Phiel [a,b], Heithem M. El-Hodiri [a,b], Jing Yang [a,b,*]

[a] *Columbus Children's Research Institute, USA*
[b] *Department of Pediatrics, The Ohio State University, 700 Children's Drive, Columbus, OH 43205, USA*

Received for publication 19 September 2006; revised 29 September 2006; accepted 5 October 2006
Available online 10 October 2006

Abstract

Eye induction and eye field separation are the earliest events during vertebrate eye development. Both of these processes occur much earlier than the formation of optic vesicles. The insulin-like growth factor (IGF) pathway appears to be essential for eye induction, yet it remains unclear how IGF downstream pathways are involved in eye induction. As a consequence of eye induction, a single eye anlage is specified in the anterior neural plate. Subsequently, this single eye anlage is divided into two symmetric eye fields in response to Sonic Hedgehog (Shh) secreted from the prechordal mesoderm. Here, we report that B56ε regulatory subunit of protein phosphatase 2A (PP2A) is involved in *Xenopus* eye induction and subsequent eye field separation. We provide evidence that B56ε is required for the IGF/PI3K/Akt pathway and that interfering with the PI3K/Akt pathway inhibits eye induction. In addition, we show that B56ε regulates the Hedgehog (Hh) pathway during eye field separation. Thus, B56ε is involved in multiple signaling pathways and plays critical roles during early development.

Keywords: B56ε; PP2A; Eye induction; Eye field separation; IGF; Hh

Introduction

Vertebrate eye development starts at gastrulation when the eye field is specified in the anterior neural plate. Subsequently, the eye field is divided into two in response to an inhibitory signal secreted from the prechordal plate. Both eye induction and eye field separation have already been completed by the time optic vesicles become morphologically visible (for review, see Chow and Lang, 2001).

Proper eye development relies on the precise expression of eye field transcription factors (EFTFs) (Chow and Lang, 2001; Zuber et al., 2003). Although these genes may be induced through distinct mechanisms (Oliver et al., 1995; Stoykova et al., 1996; Zhang et al., 2000), they are expressed largely in an overlapping pattern. EFTFs are capable of inducing ectopic eye formation in misexpression experiments. In addition, mutations in EFTFs cause abnormal eye development. Interestingly, EFTFs regulate the expression of each other (Ashery-Padan and Gruss, 2001; Bailey et al., 2004; Chow and Lang, 2001). Several signaling pathways have been found to be essential for early eye development. These include the IGF pathway (Eivers et al., 2004; Pera et al., 2003; Pera et al., 2001; Richard-Parpaillon et al., 2002), the Wnt pathway (Cavodeassi et al., 2005; Rasmussen et al., 2001; Van Raay et al., 2005), and the planar cell polarity (PCP) pathway (Lee et al., 2006; Maurus et al., 2005; Moore et al., 2004). Among these, IGF, a potent neural and forebrain inducer, is sufficient and necessary for eye induction. In *Xenopus* and *Zebrafish*, ectopic activation of the IGF pathway induces the expression of EFTFs and highly organized ectopic eyes. Conversely, interfering with IGF signaling blocks eye induction (Eivers et al., 2004; Pera et al., 2003; Pera et al., 2001; Richard-Parpaillon et al., 2002). Recently, it has been shown that *Kermit2*, an IGF receptor binding protein, plays a role during *Xenopus* eye development (Wu et al., 2006). Although the function of IGF signaling during mammalian eye induction has not been studied, several IGF pathway components are expressed at very high levels in rat early retina progenitors (James et al., 2004). This suggests that

* Corresponding author. Department of Pediatrics, The Ohio State University, 700 Children's Dr., Columbus, OH 43205, USA. Fax: +1 614 722 5892.
E-mail address: yangj@ccri.net (J. Yang).

0012-1606/$ - see front matter © 2006 Elsevier Inc. All rights reserved.
doi:10.1016/j.ydbio.2006.10.011

the IGF pathway may be essential for mammalian eye induction as well. In many experimental contexts, IGF activates the PI3K/Akt and MAPK pathways (Oldham and Hafen, 2003). The MAPK pathway has been shown to be important for neural induction (Pera et al., 2003; Pera et al., 2001; Stern, 2005). However, it remains unclear how IGF downstream pathways are involved in eye induction.

After eye induction, EFTFs are expressed as a single domain in the anterior neural plate. In many species, EFTFs expression domain is subsequently divided into two by Shh secreted from the prechordal plate (Ekker et al., 1995; Li et al., 1997; Marti et al., 1995; Shimamura et al., 1995), leading to the formation of two symmetric eye primordia (Chow and Lang, 2001; Li et al., 1997). In agreement with the role of Shh in the eye field separation, cyclopia or holoprosencephaly has been found in: human patients with reduced Shh signaling (Roessler et al., 1996; Wallis and Muenke, 2000); mice lacking *Shh* (Chiang et al., 1996), *Smoothened* (*Smo*) (Zhang et al., 2001), or *Dispatched* (Ma et al., 2002); animals exposed to the Hh inhibitor, cyclopamine, during embryonic development (Keeler, 1970) and *Xenopus* or chick embryos with the prechordal mesoderm physically removed (Li et al., 1997). Interestingly, *Zebrafish* eye field separation process relies more on the medial lateral movement of retina precursor cells (Woo and Fraser, 1995; Woo et al., 1995; Rembold et al., 2006). Mutants exhibiting abnormal cell movement show various degrees of cyclopia (Hammerschmidt et al., 1996; Heisenberg et al., 1996; Heisenberg and Nusslein-Volhard, 1997; Marlow et al., 1998; Solnica-Krezel et al., 1996).

PP2A is one of a serine/threonine protein phosphatases abundantly expressed and is involved in numerous biological processes. The PP2A holoenzyme consists of a catalytic subunit (C), a structural subunit (A), and a regulatory subunit (B). The activity and specificity of PP2A are regulated by its regulatory subunits. Three PP2A regulatory subunit families, B55, B56, and PR72, have been identified (Janssens and Goris, 2001). Among these, the B56 family (McCright and Virshup, 1995) comprises the largest regulatory subunit family. Five B56 family members have been identified in mammals, including α, β, γ, δ, and ε. B56 family members have been implicated in the canonical Wnt pathway (Gao et al., 2002; Li et al., 2001; Ratcliffe et al., 2000; Seeling et al., 1999; Yang et al., 2003), the PCP pathway (Hannus et al., 2002), and are required for cell survival (Hannus et al., 2002; Li et al., 2002; Silverstein et al., 2002). Our previous studies have shown that B56ε is required for the Wnt pathway during *Xenopus* axis specification and midbrain–hindbrain boundary formation (Yang et al., 2003). Here, we report that B56ε is required for the IGF/PI3K/Akt and the Hh pathways. B56ε is involved in eye induction and eye field separation during *Xenopus* development.

Materials and methods

Oocyte and embryo manipulations

Xenopus oocytes and embryos were obtained as described (Sive et al., 2000). Host transfer, regular microinjection, and animal cap assays were performed as described (Yang et al., 2003). For 32-cell stage injection, 5 nl of solution was injected. The dosage of RNA or morpholino for microinjection was indicated in the text or figure legend. For experiments in which RNA and morpholino were injected into the same embryo, RNA and morpholino were injected sequentially. For LY294002 treatment, animal caps were exposed to various concentrations of the drug from stage 9 to stage 13.

Plasmid construction and morpholino

FLAG-costal2 was generated by PCR from *zebrafish costal2* (Tay et al., 2005). *Gli-VP* was constructed by cloning a PCR fragment containing the zinc finger of *Xenopus Gli1* to the pCS2-VP16 vector (GCCACTCGAGAATT-CTGGCTTGGATACGATTGGG and GGAGCTCGAGTCTAGATC-CAGCTGGTTTTCCCCTT). *Myc-EGFP* was constructed by cloning the PCR fragment of EGFP between the *Eco*RI and *Xho*I sites of pCS2-MT (ATAAA-GAATTCAATGGTGAGCAAGGGCGAGGAG and ATATCTCGAGT-TACTTGTACAGCTCGTCCATGCC). The morpholino against B56ε (εmor) and the 5-mismatched control morpholino were described (Yang et al., 2003).

RT-PCR and whole mount in situ hybridization

RNA extraction and RT-PCR method were described previously (Yang et al., 2003). PCR primers are: *sox3* (up): AGCACAGGTATGACATGAGC, *sox3* (down): ATCATATCTCGCAGGTCTCC; *shh* (up): 5′-TACTGTCTCGTCTCTACACC-3′, *shh* (down): 5′-CATCTGTCCGAGC-GAAGC-3′; *foxA2* (up): 5′-CCAGCTCCATGAACATGTCC-3′, *foxA2* (down): 5′-TCCATAAATTGGGCTCATGG-3′; and *ptc-1* (up): 5′-GGACAA-GAATCGCAGAGCTG-3′, *ptc-1* (down): 5′-GGATGCTCAGGGAACCT-TAC-3′. Primers for *dickkopf-1*, *goosecoid*, *cerberus*, *nodal-related3*, *sizzled*, *ODC*, *otx2* (Yang et al., 2003), *rx lhx2*, *pax6*, *six3*, and *ET* (Zuber et al., 2003) were described. Whole mount in situ hybridization was performed as described (Sive et al., 2000).

Western blots and Co-IP

Western blots were performed as described (Yang et al., 2003). Antibodies are anti-FLAG (M2, Sigma, 1:1000), anti-Myc (9E10, Sigma, 1:1000), anti-ERK (Transduction laboratory, 1:2500), anti-*p*-ERK (Cell Signaling, 1:1000), anti-Akt (Cell Signaling, 1:1000), and anti-*p*-Akt (Sigma, 1: 500). For Co-IP, caps were homogenized in NP-40 buffer (1× PBS, 0.1% NP-40, proteinase inhibitor cocktail; 10 μl per animal cap). Cleared lysates from a group of 15 animal caps were incubated with antibody (1:100 dilution) at room temperature for 2 h and further incubated with protein G beads for 1 h. Beads were washed with NP-40 buffer three times. Samples were boiled in 1× SDS sample buffer for 3 min and separated by SDS-PAGE.

Results

Injection of εmor causes dose-dependent eye defects

We have previously reported that depletion of *B56ε* in the neural ectoderm impairs midbrain–hindbrain boundary formation and causes eye defects (Yang et al., 2003). To further characterize the function of B56ε during *Xenopus* eye development, we injected various doses of εmor into two dorsal animal blastomeres at the 8-cell stage. Injected embryos were harvested at stage 20 and analyzed by whole mount in situ hybridization for *rx* (Mathers et al., 1997) and *six3* (Zhou et al., 2000), two definitive eye markers.

At stage 20, control embryos had two symmetric *rx* (100%, $n=57$) and *six3* (100%, $n=64$) expression domains. However, embryos injected with 2.5 ng of εmor had either a single *rx* (20%, $n=104$) and *six3* (17%, $n=86$) expression domain, or

two domains closer to the dorsal midline (not shown). Injecting 5 ng of εmor caused more severe phenotypes. Virtually all injected embryos exhibited one *rx* ($n=93$) and one *six3* ($n=112$) expression domain. In addition, the expression of *rx* (66%) and *six3* (57%) in many injected embryos was reduced. When 7.5 ng of εmor was injected, the majority of injected embryos completely lacked *rx* (74%, $n=66$) and *six3* (54%, $n=56$) expression (Fig. 1A). Thus, injection of εmor caused dose-dependent eye defects.

To address the specificity of the εmor, we took advantage of a control morpholino carrying 5 mismatched nucleotides (5mis). Injection of εmor (5 ng) caused a nearly complete blockage of *B56ε* translation. In contrast, *B56ε* translation appeared to be normal when 5 ng of 5mis was injected (Fig. 1B). We noticed that a higher dose of 5mis (20 ng) reduced the translation of *B56ε* slightly (not shown). Thus, 5mis only has minimal effect on *B56ε* translation.

Next, we injected various doses of εmor and 5mis and analyzed the effects of morpholino injection on early development. Injection of 5 ng of εmor slightly delayed blastopore closure (not shown). At the tadpole stage, 69% ($n=124$) of injected embryos failed to form eyes and developed shorter anterior–posterior (AP) axis (Fig. 1C). When 7.5 ng of εmor was injected, all injected embryos had permanent blastopore closure defects. At the tadpole stage, 86% of injected embryos ($n=107$) had severe morphogenesis defects and essentially all injected embryos lacked eye formation. Injection of 5mis only caused minimal developmental defects. Embryos injected with 5 ng of 5mis developed normally ($n=77$, Fig. 1C). When 7.5 ng of 5mis was injected, all injected embryos had normal blastopore closure. At the tadpole stage, 7% of embryos exhibited fused eyes (not shown), 67% of embryos developed slightly reduced eyes (as shown in Fig. 1C), and the remaining 26% of embryos were normal ($n=96$). We also analyzed *rx* and *six3* expression in 5mis injected embryos. Similar to control embryos, embryos injected with 5 ng of 5mis exhibited two separate *rx* ($n=41$) and *six3* ($n=46$) expression domains at stage 18 (Fig. 1D). Injection of 7.5 ng of 5mis affected *rx* and *six3* expression weakly, with 14% of embryos ($n=47$) exhibiting fused *rx* expression domains, and 29% of embryos ($n=48$) exhibiting fused *six3* expression domains (Fig. 1D). Thus, injection of mismatched control morpholino only induced minimal eye defects. Taken together, the above results indicate that depletion of *B56ε* by εmor injection affects the expression of EFTFs and eye development.

In *Xenopus*, weak ventralization results in cyclopia, or embryos without eyes (De Robertis and Kuroda, 2004; Harland and Gerhart, 1997; Heasman, 1997; Kao and Elinson, 1988; Xanthos et al., 2002). We have previously shown that maternal depletion of *B56ε* (by injecting 2.5 to 5 ng of εmor into *Xenopus* oocyte and following with host transfer procedure) resulted in ventralized embryos (Yang et al., 2003). To address whether the eye defects observed in εmor injected embryos are caused by ventralization, we compared the effects of oocyte injection (maternal depletion) and 8-cell stage injection on axis specification. Consistent with our previous observation, injection of 5 ng of εmor into oocyte resulted in ventralized embryos. When analyzed at early gastrula stage, the expression of organizer genes was severely reduced. These include *dickkopf-1* (Glinka et al., 1998), *cerberus* (Bouwmeester et al., 1996), *goosecoid* (Cho et al., 1991) and *nodal-related3* (Smith et al., 1995). The expression of *sizzled* (Salic et al., 1997), a ventral specific gene, was up-regulated. In contrast to maternal depletion of *B56ε*, *sizzled* and organizer genes were expressed normally in embryos injected with 7.5 ng of εmor at the 8-cell stage (Fig. 2A). We also analyzed the spatial expression pattern of *chordin* (*chd*) (Sasai et al., 1994), another organizer gene, in embryos injected with εmor at the 8-cell stage. Compared to control embryos ($n=67$), the expression of *chd* was normal in all εmor injected embryos ($n=83$, Fig. 2B). Thus, injection of εmor at the 8-cell stage impairs the expression of eye markers without ventralizing embryos.

We also noticed that higher doses of εmor injection caused blastopore closure defects. It is known that gastrulation defects may indirectly affect eye development. To address whether *B56ε* plays a direct role during eye development, we injected various doses of εmor into a dorsal animal blastomere (A1), which later gives rise to the anterior neural ectoderm (Moody, 1987a,b), at the 32-cell stage. Under this condition, injected embryos did not exhibit blastopore closure defects (not shown). When analyzed at stage 18, εmor injection resulted in dose-dependent eye defects, judged by *rx* expression (Fig. 2C). Embryos injected with 0.5 ng of εmor expressed *rx* relatively normally (90%, $n=42$). When 1 ng of εmor was injected, the level of *rx* expression was normal in 76% of injected embryos ($n=49$). However, *rx* positive cells were found to be closer to the midline (on the injected side) in 41% of the embryos. Injection of 1.5 ng of εmor reduced *rx* expression in 75% of injected embryos ($n=61$). Notably, none of these embryos completely lacked *rx* expression (not shown). This is likely because multiple blastomeres of the 32-cell stage embryo contribute to the eye (Moody, 1987b). Regardless, εmor injection impairs *rx* expression when targeted to the anterior neural ectoderm. This demonstrates that *B56ε* plays a direct role in the regulation of *rx* expression.

To better understand how B56ε regulates eye induction, we further examined whether *B56ε* depletion affects neural induction and forebrain specification. Thus, 4.5 ng of εmor was injected unilaterally at the 8-cell stage. This dose of εmor injection reduces EFTFs without significantly blocking the blastopore closure. At stage 12.5, 55% ($n=58$) of εmor injected embryos exhibited reduced *rx* expression on the injected side. In contrast, εmor injection did not significantly alter the expression of *sox3* (100%, $n=82$), a pan-neural marker (Penzel et al., 1997); and *otx2* (94%, $n=47$), a forebrain marker (Pannese et al., 1995) (Fig. 2D). This indicates that neural induction and forebrain specification occurred in *B56ε* depleted embryos.

We have previously shown that *B56ε* is required for the Wnt pathway (Yang et al., 2003). As the Wnt pathway is involved in the AP patterning, we tested whether the eye defects in *B56ε* depleted embryos were caused by abnormal AP patterning within the developing brain. Thus, markers expressed in different territories of the brain were analyzed. At stage 14,

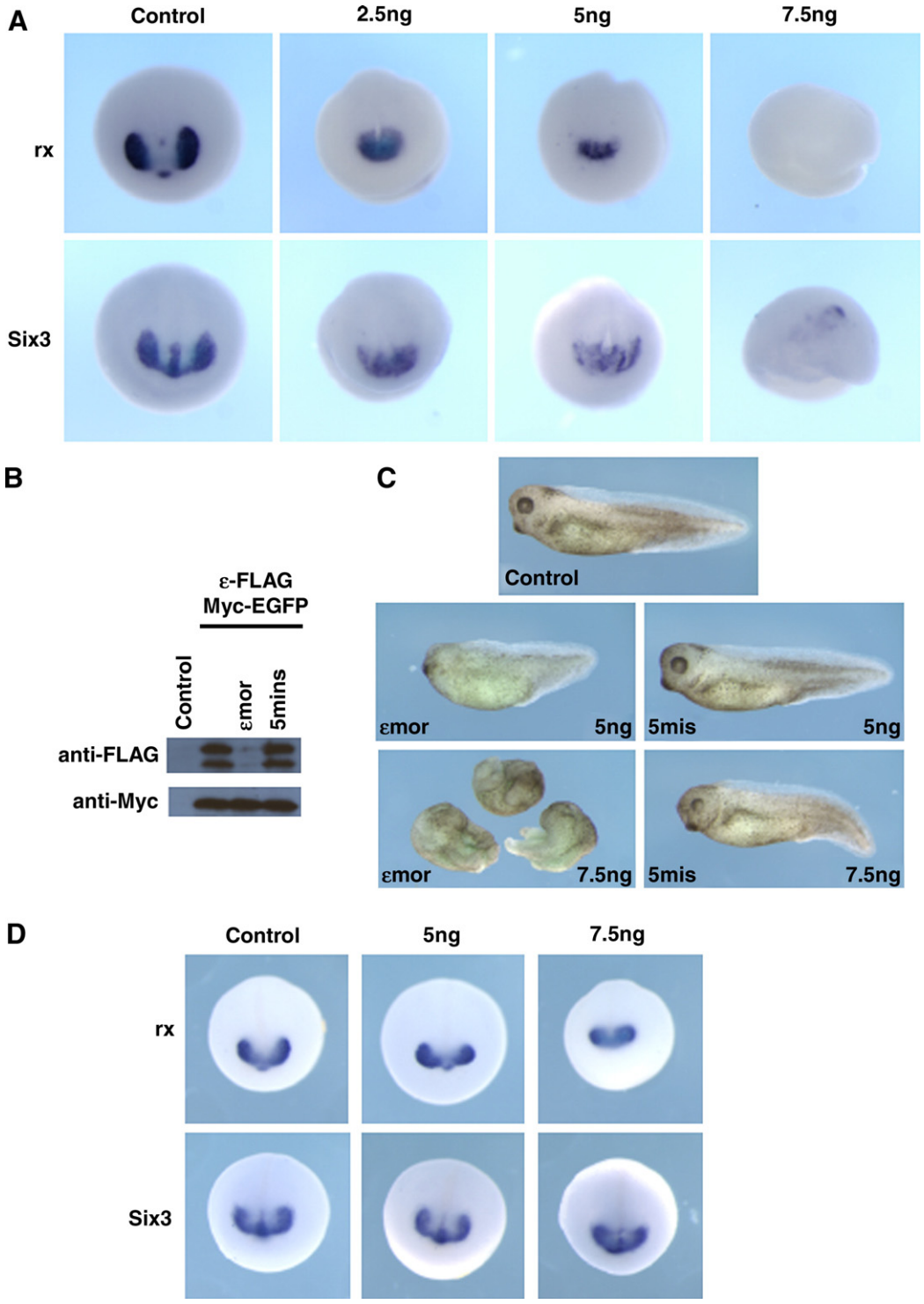

Fig. 1. Dose-dependent effects of *B56ε* depletion on eye development. (A) Whole mount in situ hybridization showing the expression of *rx* (upper panels) and *six3* (lower panels) in stage 20 control embryos, 2.5 ng εmor injected embryos, 5 ng εmor injected embryos, and 7.5 ng εmor injected embryos. εmor was injected into two dorsal animal blastomeres at the 8-cell stage. (B) Western blot showing the effects of εmor and 5mis on the translation of *B56ε-FLAG*. Myc-EGFP was used as a control for injection and loading. Morpholinos (5 ng) were injected into one of the dorsal animal blastomere at the 8-cell stage. Subsequently, a mixture of *B56ε* (200 pg) and Myc-EGFP (50 pg) was injected into the same blastomere. Injected embryos were harvested at the late gastrula stage. (C) Whole embryo phenotypes at the tadpole stage showing the effect of morpholinos injection on early embryonic development. Embryos were either uninjected (top), or bilaterally injected with εmor (5 ng, middle left; 7.5 ng, lower left), or injected with 5mis (5 ng, middle right; 7.5 ng, lower right) into both dorsal animal blastomeres at the 8-cell stage. (D) Whole mount in situ hybridization showing the expression of *rx* (upper panels) and *six3* (lower panels) in stage 18 control embryos, 5 ng of 5mis injected embryos, and 7.5 ng of 5mis injected embryos. 5mis was injected into two dorsal animal blastomeres at the 8-cell stage. Note that less than 30% of embryos injected with 7.5 ng of 5mis exhibited fused *rx* or *six3* expression at this stage. The rest of embryos were normal (not shown).

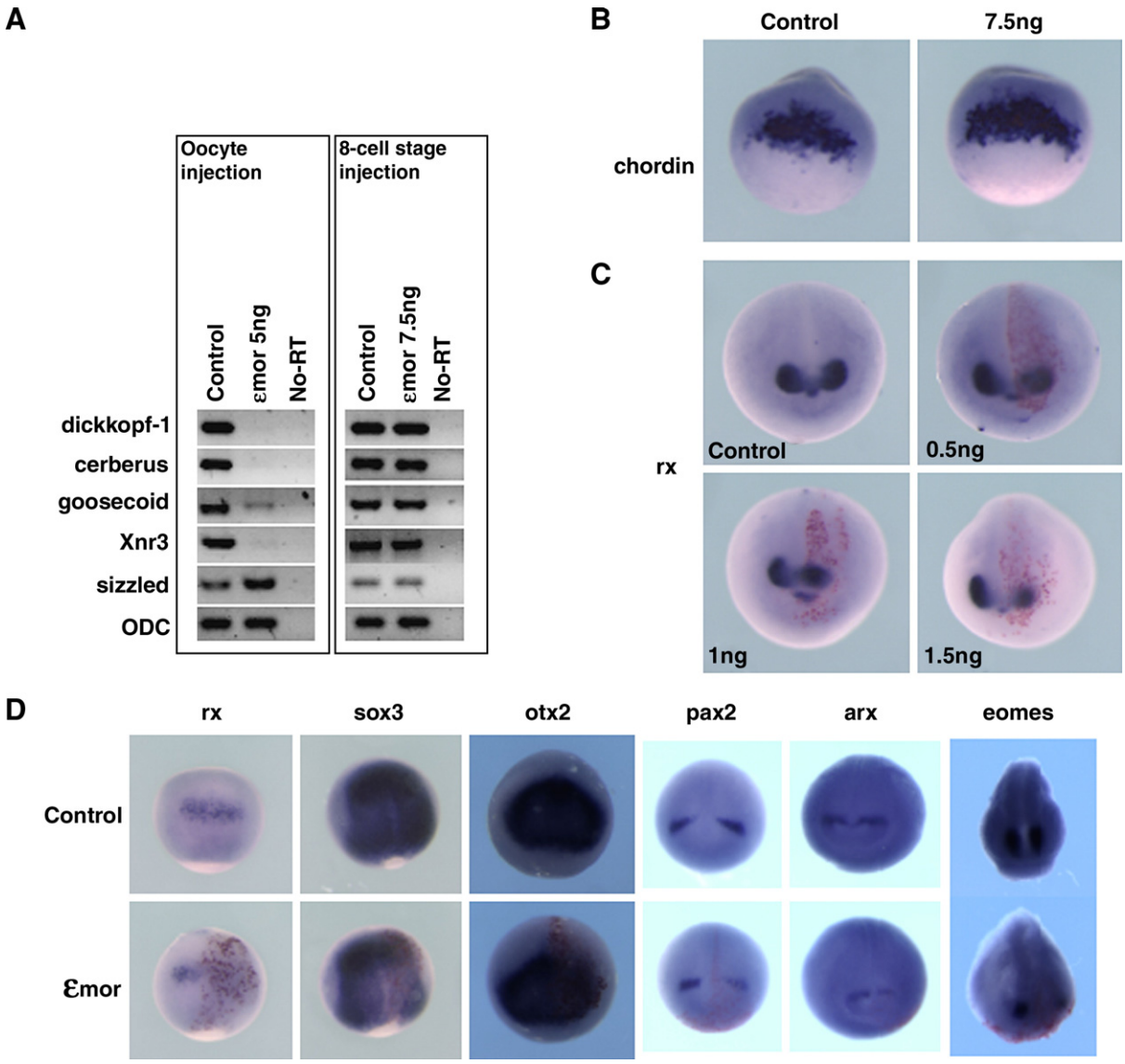

Fig. 2. B56ε plays a direct role in the regulation of *rx* expression. (A) RT-PCR showing that maternal depletion of *B56ε* (oocyte injection) reduced the expression of dorsal specific genes (*dickkopf-1*, *goosecoid*, *cerberus*, and *Xenopus nodal related3* (*xnr3*)) and enhanced the expression of a ventral-specific gene (*sizzled*) at stage 11. Injection of 7.5 ng of εmor into two dorsal animal blastomeres at the 8-cell stage did not affect the expression of above genes. *ODC* was used as the loading control. (B) Whole mount in situ hybridization showing that the expression of *chd* in a control embryo and an embryo injected with 7.5 ng of εmor. (C) Whole mount in situ hybridization showing the expression of *rx* in a stage 18 uninjected embryo, an embryo injected with 0.5 ng of εmor, an embryo injected with 1 ng of εmor, and an embryo injected with 1.5 ng of εmor. εmor was injected into one of A1 blastomeres at the 32-cell stage. Lineage tracer, *n-β-gal*, was co-injected with εmor to indicate the side of injection. (D) Whole mount in situ hybridization showing the expression of *rx* (stage 12.5), *sox3* (pan-neural, stage 12.5), *otx2* (pan-forebrain, stage 12.5), and *pax2* (midbrain, stage 14), *arx* (diencephalons, stage 14), and *eomesodermin* (telencephalon, stage 26/27) in control embryos (upper panels) and embryos injected with εmor (4.5 ng, lower panels). The right side was injected as indicated by the Red-gal staining. Embryos were injected unilaterally at the 8-cell stage.

pax2, a midbrain marker (Heller and Brandli, 1997), was expressed normally in 83% of εmor injected embryos ($n=47$). The remaining 17% of embryos exhibited weakly reduced *pax2* on the injected side. The expression of *arx*, a diencephalon marker (Seufert et al., 2005), was reduced by εmor injection in 48% of injected embryos ($n=42$). When analyzed at stage 26/27, 53% of εmor injected embryos ($n=40$) had reduced expression of *eomesodermin,* a telencephalon marker (Ryan et al., 1998), on the injected side (Fig. 2D). The expression of *meis3*, a hindbrain and spinal cord marker (Salzberg et al., 1999), was normal in εmor injected embryos (not shown). Notably, despite εmor injection reduced some of these brain markers to various degrees, we failed to observe any expansion of posterior markers in εmor injected embryos. Therefore, it is unlikely that the eye development defects in B56ε depleted embryos are caused by abnormal AP patterning, although this data suggests that B56ε may be involved in telencephalon and diencephalon development.

B56ε is required for the initiation of a subset of EFTFs

EFTFs regulate the expression of each other (Ashery-Padan and Gruss, 2001; Bailey et al., 2004; Chow and Lang, 2001). In principle, the loss of EFTFs expression in εmor injected

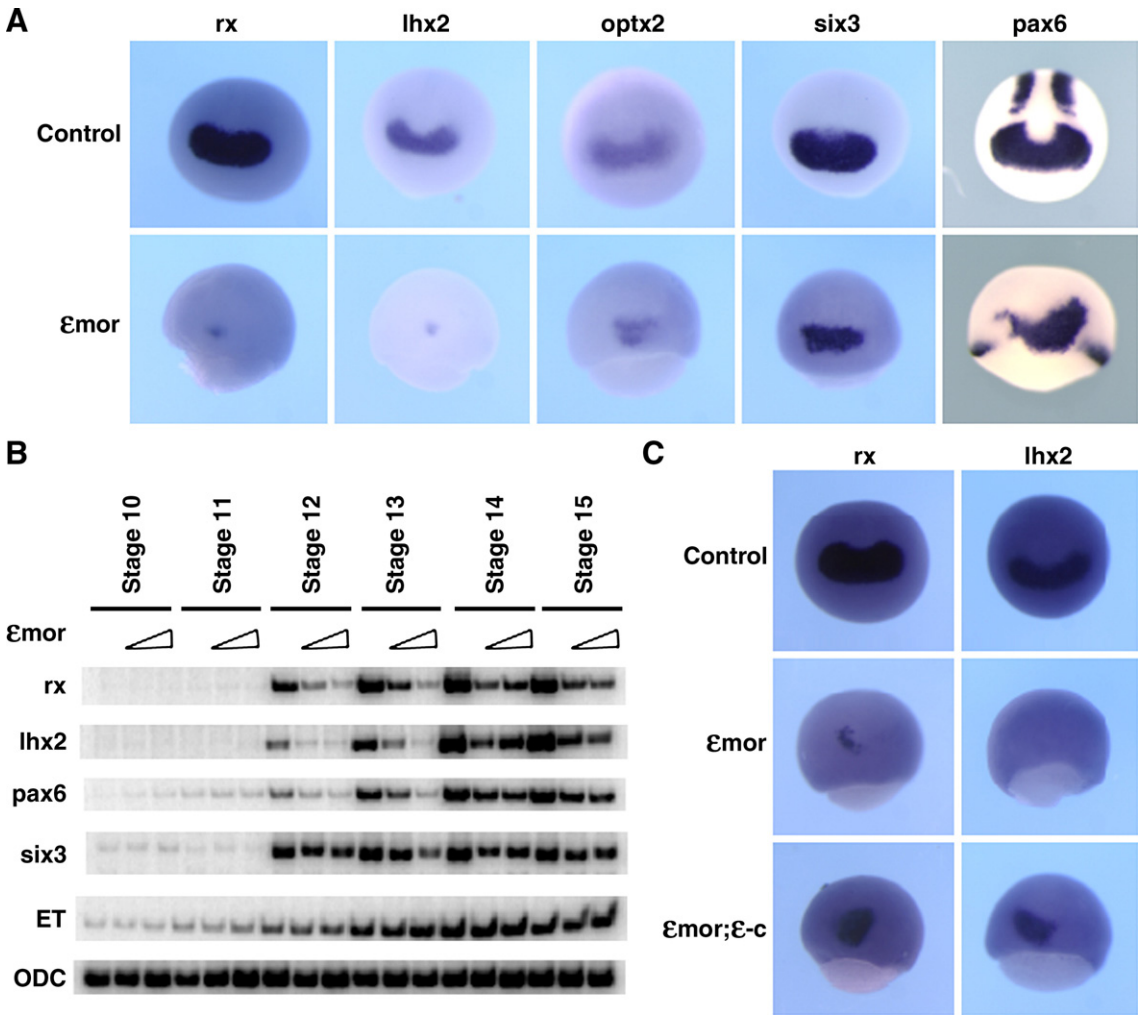

Fig. 3. B56ε is required for the induction of a subset of EFTFs. (A) Whole mount in situ hybridization showing the expression of *rx*, *lhx2*, *optx2*, *six3*, and *pax6* in stage 14 uninjected embryos (upper panels) and embryos bilaterally injected with 7.5 ng of εmor (lower panels). (B) RT-PCR showing the expression of *rx*, *lhx2*, *pax6*, *six3*, and *ET* in control embryos, embryos bilaterally injected with 5 ng or 7.5 ng of εmor from stage 10 (the beginning of gastrulation) to stage 15 (mid-neurula stage). *ODC* was used as loading control. (C) Whole mount in situ hybridization showing the expression of *rx* (left column) and *lhx2* (right column) in stage 14 uninjected embryos (upper panels), embryos injected with εmor (7.5 ng, middle panels), and embryos injected with εmor (7.5 ng) and ε-*c* (100 pg) (lower panels). Both dorsal animal blastomeres were injected at the 8-cell stage. Morpholino and ε-*c* were injected sequentially. Note that the expression of *rx* and *lhx2* was partially rescued by ε-*c*.

embryos may be caused by the lack of the entire eye field, or due to the failure of a subset of EFTFs expression within the eye field. To distinguish between these possibilities, embryos were bilaterally injected with 7.5 ng of εmor, a dose of εmor sufficient for a complete blockage of eye development. Injected embryos were analyzed by whole mount in situ hybridization and RT-PCR for EFTFs, including *rx*, *lhx2* (Bachy et al., 2001), *optx2* (Zuber et al., 1999), *six3*, *pax6*, and *ET* (Li et al., 1997).

At stage 14, *rx*, *lhx2*, *optx2*, *six3,* and *pax6* were expressed as a single domain in the developing eye field in control embryos. Embryos injected with 7.5 ng of εmor, however, exhibited severely reduced *rx* (71%, $n=97$) and *lhx2* (82%, $n=45$) expression. The expression of *optx2* (80%, $n=41$), *six3* (82%, $n=38$) and *pax6* (75%, $n=44$) was only moderately down-regulated (Fig. 3A). This expression profile was further confirmed by RT-PCR. The expression of *rx*, *lhx2*, *pax6*, and *six3* was initiated at stage 12. At this stage, injection of 5 ng and 7.5 ng of εmor severely reduced the expression of *rx* and *lhx2*. In contrast, the expression of *six3* and *pax6* was only slightly decreased. The expression of *ET* was not significantly affected (Fig. 3B).

The reduction of *rx* and *lhx2* by εmor injection is due to the loss of endogenous B56ε. When εmor was injected alone, 67% ($n=55$) and 66% ($n=50$) of injected embryos failed to express *rx* and *lhx2*, respectively. The expression of *rx* and *lhx2* was partially rescued in embryos injected with εmor and ε-*c* RNA, a modified *B56ε* construct that lacks the εmor binding sequence (Yang et al., 2003). Only 33% ($n=57$) and 39% ($n=54$) of injected embryos lacked *rx* and *lhx2* expression, respectively. The blastopore closure phenotype was not rescued by ε-*c* RNA injection (Fig. 3C). Taken together, the above results demonstrate that B56ε is required for the initiation of a subset of EFTFs, suggesting a role of B56ε in eye induction.

B56ε is required for IGF1-induced EFTF expression

IGF signaling is important for eye induction (Eivers et al., 2004; Pera et al., 2001; Richard-Parpaillon et al., 2002). Since depletion of B56ε blocks the initiation of some EFTFs, we tested whether B56ε functions downstream of IGF during eye induction. Thus, we examined if εmor injection blocks IGF1-induced EFTFs expression in whole embryos and animal caps.

Compared to control embryos, overexpression of IGF1 induced ectopic expression of *rx* (51%, $n=51$), *otx2* (82%, $n=45$), and *sox3* (96%, $n=52$) in whole embryos. Depletion of *B56ε* results in a nearly complete blockage of endogenous and IGF1-induced *rx* expression (96%, $n=47$). In contrast, IGF1 still induced ectopic expression of *otx2* (74%, $n=46$) and *sox3* (91%, $n=46$) in εmor injected embryos (Fig. 4A). In animal caps, IGF1 induced the expression of *rx*, *pax6*, *lhx2*, *six3*, *sox3*, and *otx2*. Injection of εmor blocked IGF1-induced *rx*, *pax6*, *lhx2*, and *six3*, but not *sox3* or *otx2* (Fig. 4B). These results demonstrate that B56ε is required for the EFTFs induction activity of IGF1, but not for the neural and forebrain induction activity of IGF1.

The PI3K/Akt pathway is required for IGF1-induced EFTFs expression

IGF activates the PI3K/Akt pathway and the MAPK pathway in most experimental contexts (Oldham and Hafen, 2003). Since B56ε is required for IGF1-induced EFTFs expression, we further investigated whether B56ε is required for IGF1-induced Akt and MAPK signaling. Activation of the Akt pathway and the MAPK pathway was determined by monitoring endogenous Akt phosphorylation (Ser473) and ERK phosphorylation (Thr183 and Tyr185), respectively.

As shown in Fig. 5A, IGF1-induced ERK phosphorylation and Akt phosphorylation in animal caps. Injection of εmor reduced IGF1-induced Akt phosphorylation, but had no effect on IGF1-induced ERK phosphorylation, indicating that B56ε is required for the PI3K/Akt pathway, but not the MAPK pathway. To determine at which level B56ε functions in the PI3K/Akt pathway, we tested if B56ε is required for Akt phosphorylation induced by P110*, a constitutively active PI3K (Carballada et al., 2001). Overexpression of P110* induced Akt phosphorylation in animal caps. P110*-induced Akt phosphorylation was not sensitive to εmor injection, demonstrating that B56ε is required for the PI3K/Akt pathway upstream of, or at the parallel level of, PI3K.

The observations that B56ε is required for eye induction and PI3K/Akt signaling immediately suggest that the PI3K/Akt pathway is essential for eye induction. To address this, we examined whether the PI3K/Akt pathway is required for IGF1-induced EFTFs expression in animal caps and whole embryos.

As expected, overexpression of IGF1 in animal caps induced *rx*, *pax6*, *lhx2*, *six3*, *otx2*, and *sox3*. Addition of 2.5 nM of LY294002, a chemical PI3K inhibitor, reduced the IGF1-induced EFTFs expression without affecting the expression of *otx2* and *sox3* (Fig. 5B). Similarly, overexpression of IGF1 induced ectopic expression of *rx* (49%, $n=41$), *otx2* (62%,

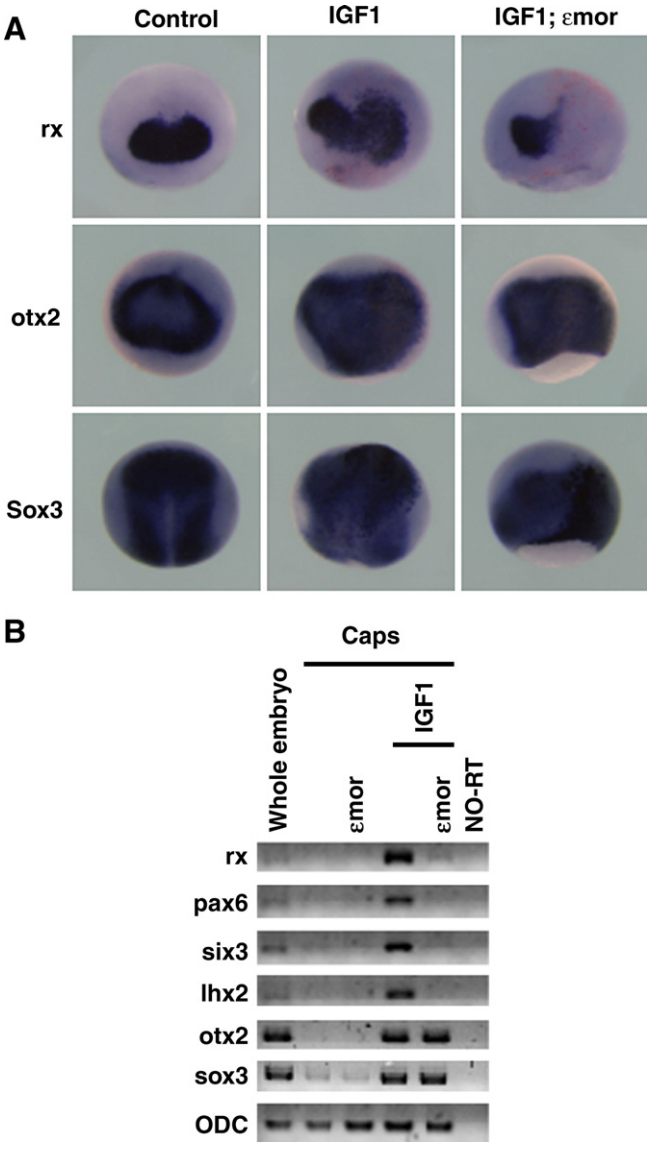

Fig. 4. B56ε is required for IGF1-induced EFTFs expression. (A) Whole mount in situ hybridization showing that εmor injection blocked IGF1-induced *rx* expression (upper panels), without affecting IGF1-induced *otx2* (middle panels) and *sox3* (lower panels) expression in whole embryos (stage 14). IGF1 (2 ng) was unilaterally injected at the 8-cell stage into either wild-type embryos, or embryos that were previously injected with 5 ng of εmor. The right side was injected. (B) RT-PCR showing εmor injection blocked IGF1-induced *rx*, *pax6*, *six3*, and *lhx2* expression, while IGF1-induced *otx2* and *sox3* expressions remain unaffected. εmor (10 ng) was injected at the 1-cell stage. IGF1 (2 ng) was radially injected into the animal pole of each blastomere at the 4-cell stage. Animal caps were dissected at late blastula stage and harvested at stage 13.

$n=55$), and *sox3* (96%, $n=52$) in whole embryos. Co-injection of IGF1 with Δp85, a dominant negative regulatory subunit of PI3K (Carballada et al., 2001), or a kinase dead Akt (dnAkt) severely blocked IGF1-induced *rx* expression (76%, $n=41$ and 90%, $n=41$, respectively). Notably, Δp85 and dnAkt not only reduced IGF1-induced *rx*, but also blocked endogenous *rx*. Consistent with the results from the animal cap assay, ectopic *otx2* expression was detected in 61% ($n=44$) of embryos injected with IGF1 and Δp85, and in 60% ($n=40$) of embryos injected with IGF1 and dnAkt. IGF1 still induced ectopic *sox3*

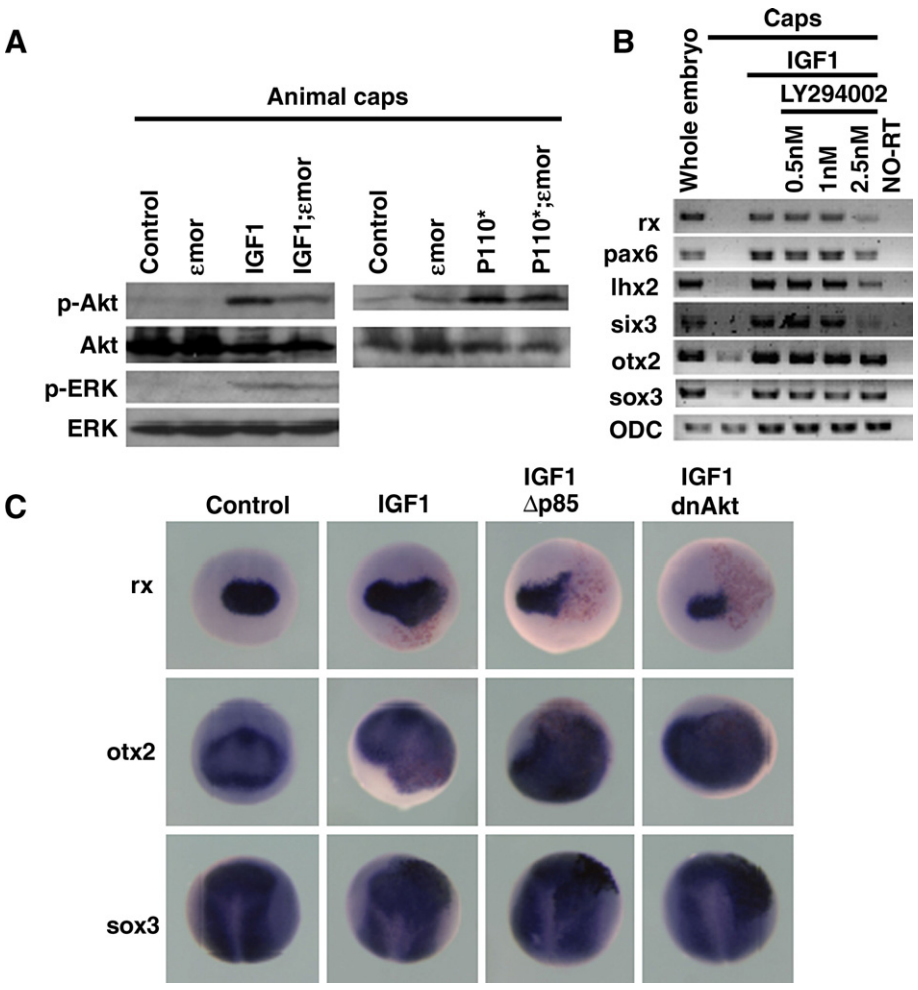

Fig. 5. The PI3K/Akt pathway is required for IGF1-induced EFTFs. (A) Western blot showing that εmor injection blocked Akt phosphorylation induced by IGF1, but had no effect on Akt phosphorylation induced by P110*. In addition, εmor had no effect on IGF1-induced ERK phosphorylation. εmor (10 ng) and RNA encoding IGF1 (2 ng) or P110* (1 ng) were injected sequentially, with εmor being injected at the 1-cell stage and RNAs being injected at the 4-cell stage. Animal caps were dissected at stage 8/9 and harvested at stage 13. (B) RT-PCR results showing LY294002, a PI3K inhibitor, blocked IGF1-induced expression of *rx*, *lhx2*, *pax6*, and *six3*, without affecting IGF1-induced *otx2* and *sox3* expressions in animal cap assay. IGF1 was injected as described above. Caps were dissected at late blastula stage and harvested at stage 13. Some caps were exposed to LY294002 from stage 9. (C) Δp85 (2 ng) and dnAkt (2 ng) blocked IGF1 (2 ng) induced *rx* (upper panels), but not IGF1-induced *otx2* (middle panels) and *sox3* (lower panels) in whole embryos. One of the dorsal animal blastomeres was injected at the 8-cell stage. The right side was injected.

expression in the presence of Δp85 or dnAkt (100%, $n=42$ and 94%, $n=52$, respectively. Fig. 5C). Taken together, these results indicate that PI3K/Akt signaling is required for the EFTFs induction activity of IGF1.

The PI3K/Akt pathway is required for endogenous eye induction

Δp85 and dnAkt blocked endogenous *rx* expression, suggesting that PI3K/Akt signaling is required for endogenous eye induction. However, it has been reported that interfering with the PI3K/Akt pathway impairs mesoderm formation (Carballada et al., 2001), which may indirectly affect eye development. To investigate the direct effect of PI3K/Akt inhibition on eye induction, we injected Δp85 and dnAkt into dorsal animal blastomeres at the 8-cell stage. Only embryos without blastopore closure defects were analyzed. Unlike control tadpoles, which formed two normal eyes ($n=49$), Δp85 (65%, $n=63$) and dnAkt (74%, $n=84$) injected embryos either lacked eyes completely, or had two severely reduced eyes located laterally (Fig. 6A). When analyzed at the late gastrula stage (stage 13), Δp85 injected embryos exhibited reduced *rx* (55%, $n=49$) and *lhx2* (57%, $n=46$) expression. Injection of dnAkt blocked *rx* (63%, $n=62$) and (52%, $n=57$) *lhx2* as well (Fig. 6B).

Furthermore, we injected Δp85 and dnAkt into one of the A1 blastomeres at the 32-cell stage. At the tadpole stage, embryos injected with Δp85 and dnAkt had reduced eyes on the injected side (53%, $n=118$ and 46%, $n=79$, respectively; Fig. 6C). We also analyzed the expression of *rx*, *myoD* (muscle), *otx2*, and *sox3* when injected embryos reached late gastrula stage. Injection of Δp85 caused cell-autonomous reduction of *rx* expression in 64% of embryos ($n=45$). These embryos had normal *myoD* expression on the injected side, indicating reduced *rx* expression was not caused by mesoderm defects. Injection of dnAkt had similar effects, with 58% of embryos

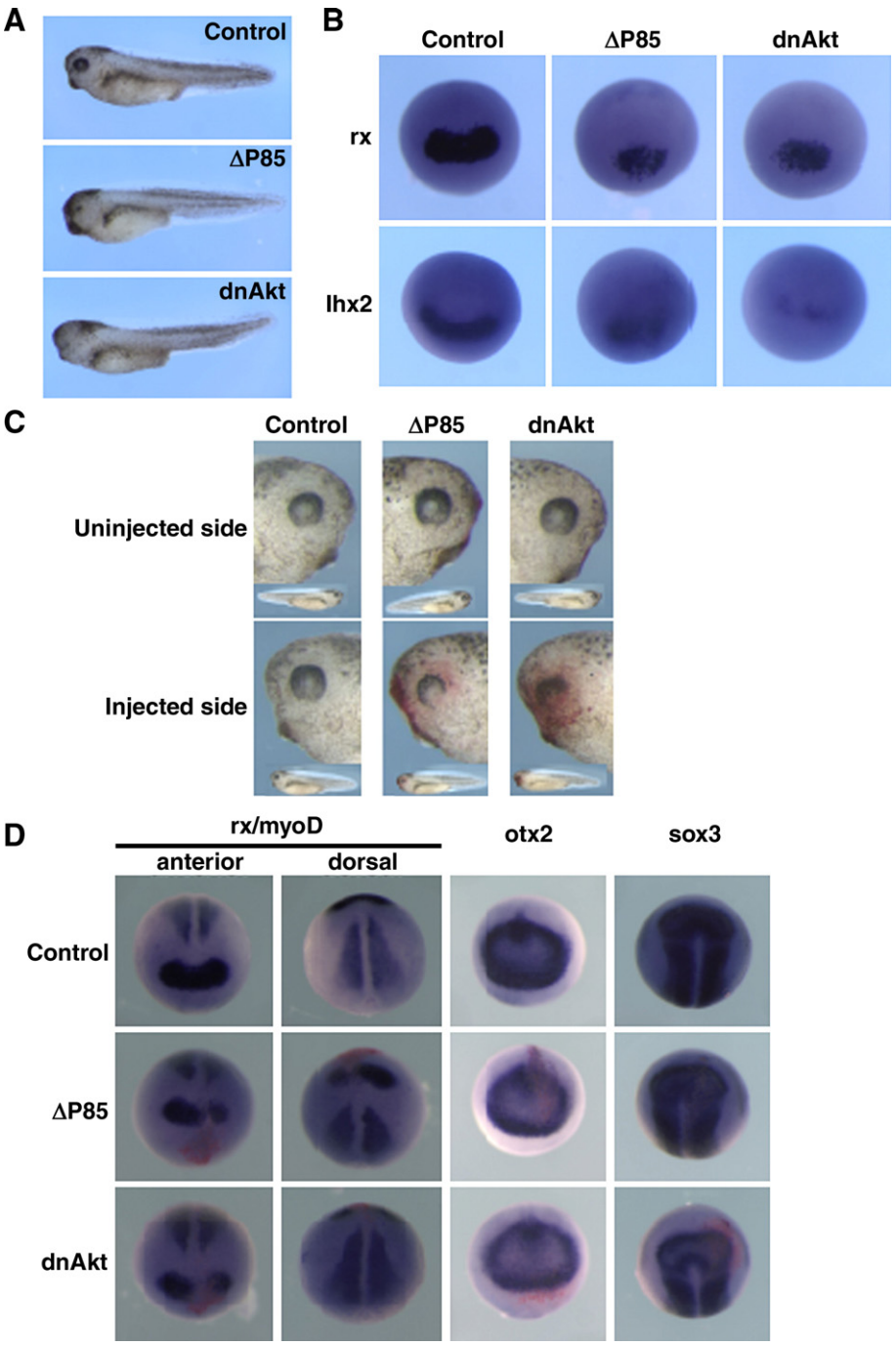

Fig. 6. The PI3K/Akt pathway is required for eye induction. (A) Injection of Δp85 (2 ng) or dnAkt (2 ng) into dorsal animal blastomeres at the 8-cell stage blocked eye formation. (B) Δp85 and dnAkt blocked the expression of *rx* (upper panels) and *lhx2* (lower panels) at stage 14. (C) Injection of Δp85 or dnAkt into A1 blastomere at the 32-cell stage impaired eye formation on the injected side (left) when embryos reached tadpole stage. Left side was injected. (D) Injection of Δp85 (middle panels) or dnAkt (lower panels) into A1 blastomere at the 32-cell stage reduced the expression of *rx*, but not *myoD*, *otx2*, and *sox3*. *n-β-gal* was used as a lineage tracer.

($n=60$) exhibiting reduced *rx* expression, while *myoD* expression was normal. The expression of *otx2* was not significantly affected by the injection of Δp85 (100%, $n=40$) or dnAkt (96%, $n=45$). In addition, injection of Δp85 ($n=41$) or dnAkt ($n=55$) did not alter the expression of *sox3* (Fig. 6D). Thus, interfering with the PI3K/Akt pathway can block eye induction without affecting mesoderm or neural/forebrain induction. Taken together, the above results indicate that the PI3K/Akt pathway is required for eye induction.

B56ε is required for eye field separation

While higher doses of εmor injection impairs eye induction, we noticed that embryos injected with lower doses of εmor formed cyclopic eyes. To further investigate the function of B56ε during eye field separation, we injected 3.5 ng of εmor into embryos. Under this condition, the majority of injected embryos developed cyclopic eyes. To determine whether the eye field separation defect in εmor injected embryos is due to

the loss of B56ε, we tested if ε-*c* RNA could rescue this phenotype in εmor injected embryos. Unlike control embryos, which formed two symmetric eyes (100%, $n=57$), 75% of εmor injected embryos ($n=64$) only formed one eye. In contrast, only 30% of embryos injected with ε-*c* and εmor were cyclopic ($n=68$, Fig. 7A). When analyzed at stage 18, control embryos developed two bilaterally located *rx* ($n=47$) and *six3* ($n=50$) expression domains. In εmor injected embryos, however, only one expression domain of *rx* (69%, $n=59$) and *six3* (66%, $n=60$) was observed. ε-*c* partially rescued this phenotype, with 57% of injected embryos having two *rx* expression domains ($n=57$) and 59% of embryos having two *six3* expression domains ($n=58$) (Fig. 7B). Therefore, we conclude that B56ε is required for eye field separation.

B56ε is required for Hh target gene expression during development

Shh signaling is essential for eye field separation. Since B56ε is required for eye field separation, we analyzed the expression of several Hh target genes in εmor injected embryos. These include *foxA2* (previously known as *hnf3β*, (Ruiz i Altaba et al., 1993; Suri et al., 2004)), a floor plate marker; *shh*, a notochord and floor plate marker (Ekker et al., 1995); and *ptc-1* and *ptc-2* (Koebernick et al., 2001; Takabatake et al., 2000), Hh receptors that are directly regulated by Hh signaling (Alexandre et al., 1996).

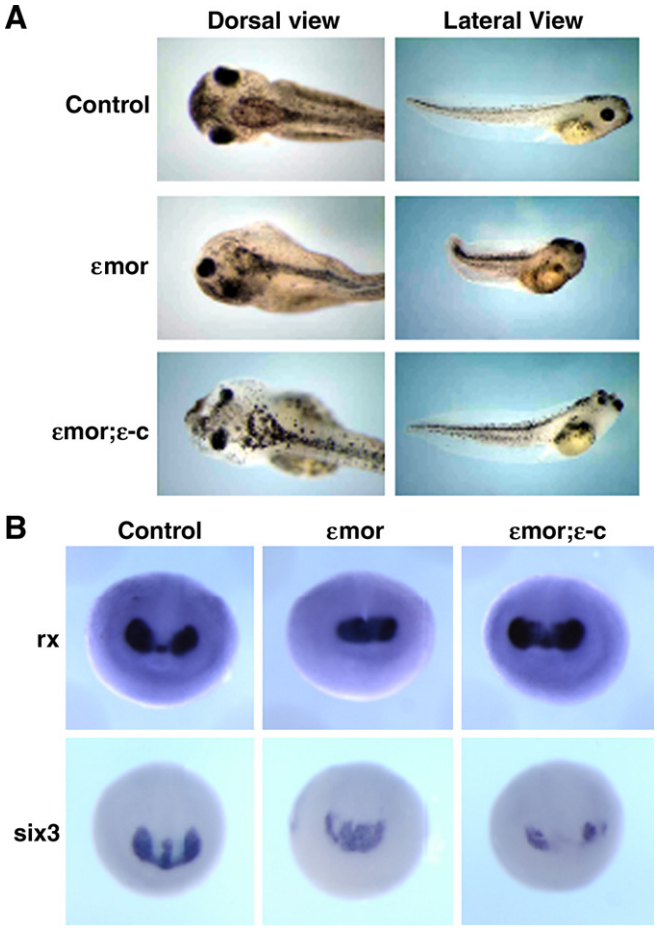

Fig. 7. B56ε is required for eye field separation. (A) Dorsal (left column) and lateral (right column) views of an uninjected embryo (upper panels), an embryo injected with εmor (3.5 ng) (middle panels), and an embryo injected with εmor and ε-*c* (100 pg) (lower panel). (B) The expression of *rx* (upper panels) and *six3* (lower panels) in stage 18 control embryos (left column), embryos injected with εmor (middle column), and embryos injected with εmor and ε-*c* (right column). Embryos were bilaterally injected at the 8-cell stage.

At stage 14/15, *shh* was expressed in the dorsal midline of control embryos (97%, $n=38$). The expression of *ptc-1* was found broadly in the anterior neural ectoderm and adjacent non-neural ectoderm (100%, $n=38$). εmor injected embryos, however, had no detectable *shh* expression (50%, $n=46$) or *ptc-1* expression (83%, $n=41$). Expression of *shh* (78%, $n=45$) and *ptc-1* (66%, $n=41$) was partially rescued by ε-*c* RNA injection (Fig. 8A). Interestingly, *shh*, *ptc-1*, and *foxA2* were initiated normally, but they were reduced in εmor injected embryos at late gastrula/early neurula stages (Fig. 8B). As the expression of Hh target genes is weak during early stages, we also analyzed Hh target gene expression at tadpole stage. Compared to control embryos, εmor injected tadpoles exhibited reduced *foxA2* (58%, $n=43$), *ptc-1* (45%, $n=44$), *ptc-2* (49%, $n=43$) and *shh* (58%, $n=45$) expression (Fig. 8C). Thus, B56ε is required for Hh target gene expression.

B56ε is required for the Hh pathway

In many species, eye field separation is regulated by Shh-mediated inhibition of EFTFs expression in the midline. Similar to the phenotypes observed in εmor injected embryos, mice embryos deficient in *shh* develop cyclopia and have reduced Hh target gene expression (Zhang et al., 2001). It is possible that the eye field separation defect in εmor injected embryos is caused by reduced *shh* transcription. To address this, we overexpressed Shh in B56ε depleted embryos and asked whether over-expressed Shh could repress EFTF expression in the midline, i.e. rescue eye field separation.

At stage 18, two completely separate *rx* expression domains were found in control embryos (100%, $n=33$). Consistent with our previous results, εmor injected embryos had only one *rx* expression domain (63%, $n=58$). When *shh* RNA was injected, *rx* expression was markedly reduced (100%, $n=43$), indicating that overexpressed Shh was sufficient for suppressing EFTF expression. Strikingly, only 54% of embryos injected with *shh* and εmor ($n=56$) exhibited reduced *rx* expression. The pattern of *rx* expression in the rest of the embryos (46%) was similar to that in εmor injected embryos. This result suggests that B56ε is required for embryos to respond to Hh signaling. To directly test this hypothesis, we examined whether Shh could induce *ptc-1*, a direct target of the Hh pathway (Alexandre et al., 1996), in *B56ε* depleted embryos at stage 14. Compared to control embryos (100%, $n=32$), εmor injected embryos exhibited reduced *ptc-1* expression (57%, $n=56$). Injection of *shh* resulted in massive ectopic *ptc-1* expression (100%, $n=54$). In contrast, overexpression of Shh in εmor injected embryos failed to induce *ptc-1* expression (51%, $n=63$) (Fig. 9A). These results indicate that B56ε may be involved the Hh pathway.

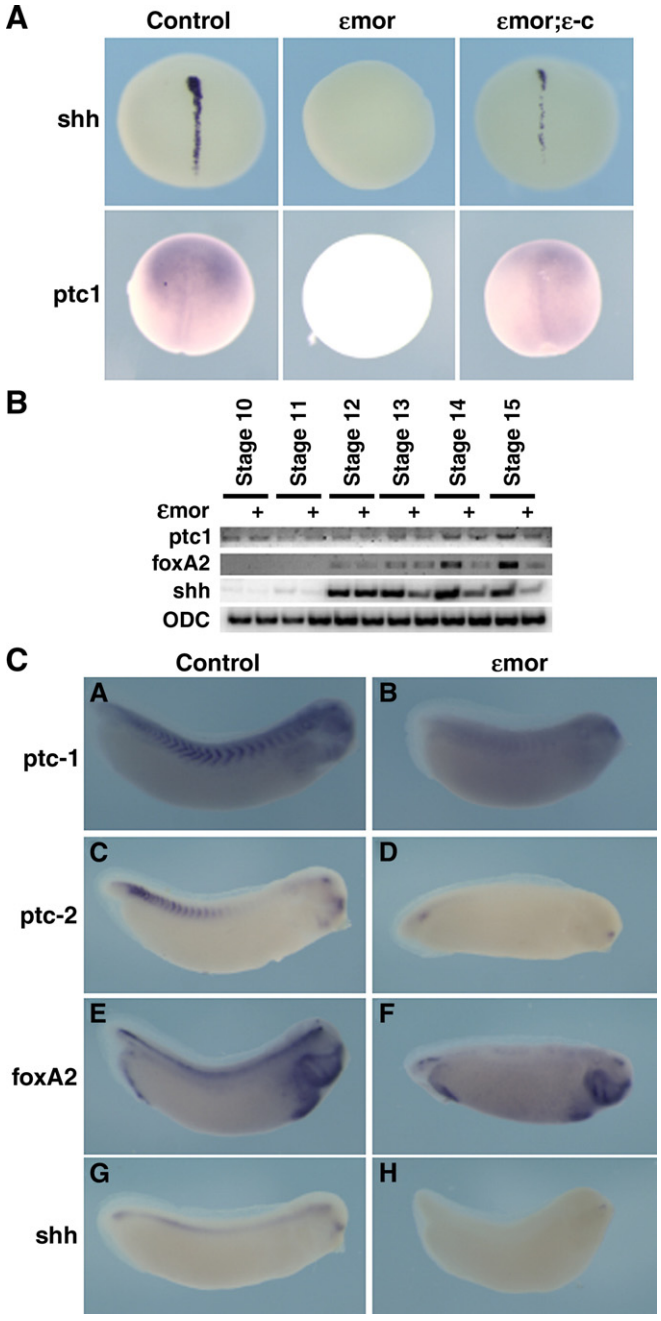

Fig. 8. B56ε is required for the expression of endogenous Hh target genes. (A) Whole mount in situ hybridization showing the expression of *shh* (upper panels) and *ptc-1* (lower panels) was reduced by εmor (3.5 ng) injection at stage 14/15. The reduced *shh* and *ptc-1* expression was partially rescued in embryos injected with εmor and ε-*c* (100 pg). (B) RT-PCR showing εmor (3.5 ng) injection reduced *ptc-1*, *foxA2*, and *shh* expression from late gastrula stage. *ODC* was the loading control. (C) The expression of *ptc-1*, *ptc-2*, *foxA2*, and *shh* in tadpole stage control embryos (left column) and embryos injected with 3.5 ng of εmor (right column). Embryos were bilaterally injected at the 8-cell stage.

The mechanism of Hh signaling has been extensively studied (Hammerschmidt et al., 1997; Huangfu and Anderson, 2006; Ingham and McMahon, 2001; McMahon et al., 2003). In *Drosophila*, Hh-dependent transcription is mediated by the zinc finger transcription factor *Cubitus interruptus* (*Ci*). In the absence of an upstream signal, *Ci* is associated with *Costal2* (*Cos2*) and is phosphorylated by several protein kinases within the *Cos2* complex. Phosphorylated *Ci* undergoes proteolytic processing, leading to the formation of a repressor form of *Ci* (Ci^R) (Aza-Blanc et al., 1997). Upon binding to *Ptc*, Hh activates *Smoothened* (*Smo*), a seven-transmembrane protein, and dissociates *Ci* from the *Cos2* complex (Zhang et al., 2005). This results in *Ci* stabilization and ultimately activates the transcription of Hh targets. Although three *Ci* homologues, *Gli1*, *Gli2*, and *Gli3*, have been identified in vertebrates, only *Gli3* undergoes pathway regulated proteolytic processing. It is generally believed that the vertebrate Hh pathway is operated similarly in *Drosophila* and vertebrates.

To further investigate the function of B56ε in the Hh pathway, we examined whether B56ε is required for Hh target gene expression induced by Shh (Ekker et al., 1995), oncogenic SmoM2 (Koebernick et al., 2003), or Gli1 (Ruiz i Altaba, 1999). As expected, Shh, SmoM2, and Gli1 (when over-expressed with *Chd*) induced *ptc-1* and *foxA2* expression in animal caps. Expression of *ptc-1* and *foxA2* induced by Shh and SmoM2 was severely reduced by εmor injection. Depletion of *B56ε* slightly inhibited Gli1-induced *ptc-1* and *foxA2* expression (Fig. 9B). To better visualize the effect of *B56ε* depletion on Gli1 activity, we used non-neuralized animal caps, which have a lower level of background *ptc-1* expression. Injection of *gli1* RNA induced *ptc-1* expression. Gli1-induced *ptc-1* expression was clearly reduced by εmor injection (Fig. 9C). In addition, we generated a constitutively active Gli1 (Gli-VP), which contains the DNA binding domain of Gli1 and the transcriptional activation domain of VP16. Overexpression of Gli-VP induced *ptc-1* expression in caps dose-dependently. The activity of Gli-VP was not sensitive to *B56ε* depletion (Fig. 9C). Therefore, these results further demonstrate that B56ε is required the Hh pathway and indicate that B56ε, likely, regulates the Hh pathway at the level of Gli.

To better understand the mechanism by which B56ε regulates the Hh pathway, we used two independent assays to test whether the Hh pathway upstream of Gli remains intact when *B56ε* is depleted. The first assay takes advantage of the observation that Gli3 undergoes proteolytic processing, which is inhibited by Shh (Wang et al., 2000). Overexpression of myc-tagged Gli3 (Ruiz i Altaba, 1999) in animal caps resulted in the expression of both full-length and truncated forms of Gli3. The truncated Gli3 was not detected when Shh was overexpressed, indicating Shh inhibited Gli3 processing. Injection of εmor did not block Shh-dependent Gli3 stabilization (Fig. 9D), demonstrating that the pathway required for Gli3 stabilization remains functional when *B56ε* is depleted. The second assay examines the interaction between Cos2 and Gli1, which is also negatively regulated by Shh. When FLAG-Cos2 and myc-Gli1 were co-expressed in animal caps, FLAG-Cos2 was pulled down by anti-myc antibody, indicating Cos2 was associated with Gli1 (Tay et al., 2005). Similar to what has been observed in *Drosophila* (Zhang et al., 2005), overexpression of Shh significantly reduced the amount of Cos2 associated with Gli1. Although εmor injection inhibited target gene expression induced by Shh, Shh still dissociated the Cos2/Gli1 complex efficiently in εmor injected caps (Fig. 9E). Therefore, the Hh

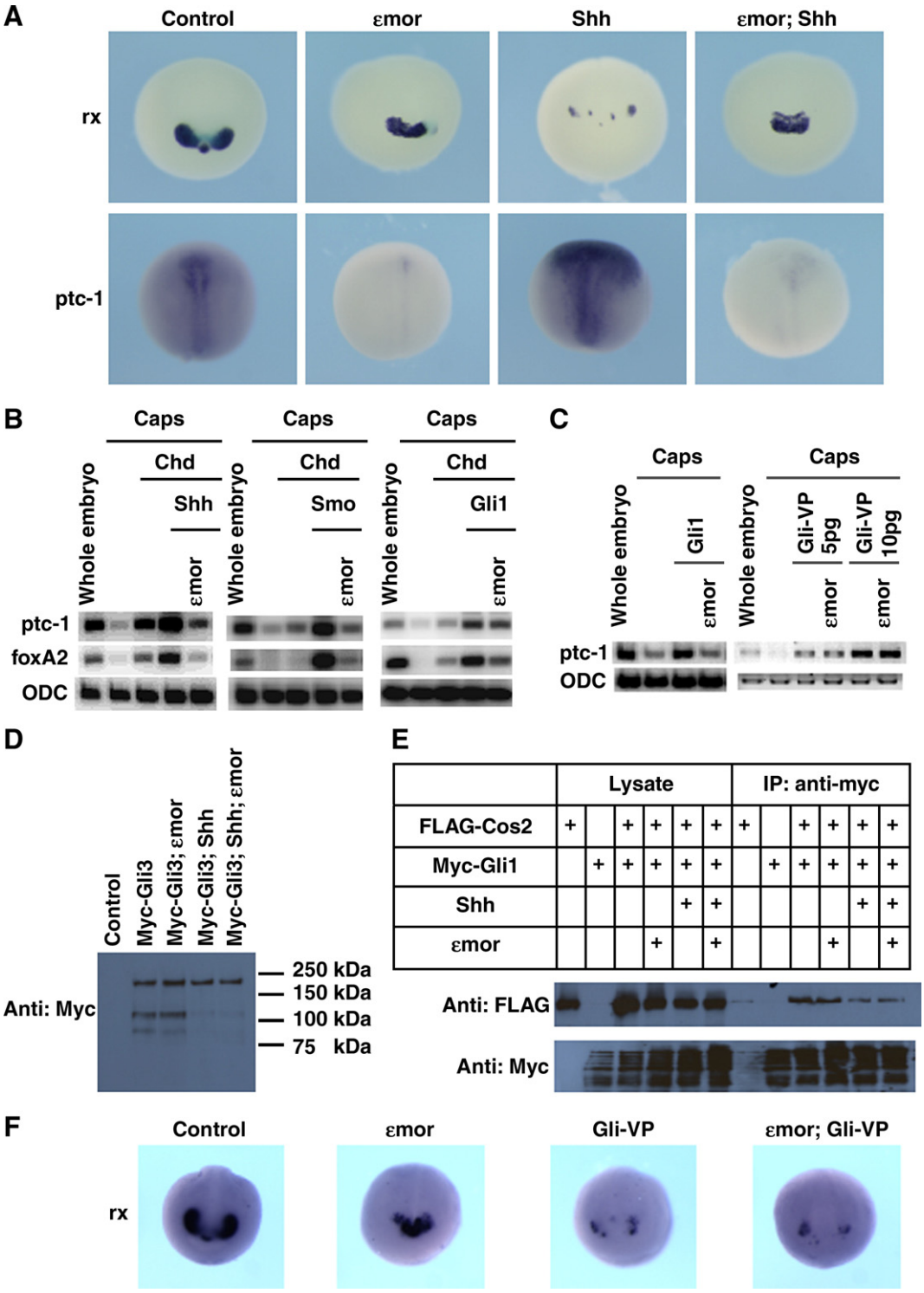

Fig. 9. B56ε is required for the Hh pathway. (A) Whole mount in situ hybridization showing εmor (3.5 ng) injection blocked *Shh* (1 ng)-induced *rx* reduction (upper panels) and *ptc-1* expression (lower panels) in whole embryos. Embryos were bilaterally injected at the 8-cell stage. (B) RT-PCR showing εmor (10 ng) injection blocked *ptc-1* and *foxA2* induced by *shh* (1 ng), *smo-M2* (2.5 ng), and *gli1* (0.5 ng) in neuralized animal caps. εmor and RNAs were injected sequentially at the 1-cell stage. Animal caps were dissected at stage 8/9 and harvested at stage 14. (C) RT-PCR showing εmor injection (10 ng) blocked *ptc-1* expression induced by wild-type *Gli1* (500 pg), but not by *Gli-VP* (50 pg and 100 pg). Embryos were injected and manipulated as described above. (D) Western blot showing overexpression of *Shh* inhibited the processing of overexpressed *Myc-Gli3* (0.5 ng) in animal caps. The effect of *Shh* (1 ng) on *Myc-Gli3* processing was not affected by εmor (10 ng) injection. Embryos were injected and manipulated as described above, except that caps were harvested at stage 12. (E) Co-IP results showing overexpression of *Shh* (1 ng) dissociated complex formation between *FLAG-Cos*2 (1 ng) and *Myc-Gli*1 (1 ng) in animal caps. Injection of εmor (10 ng) did not affect this complex dissociation induced by *Shh*. Embryos were injected and manipulated as described above. (F) Whole mount in situ hybridization showing the expression of *rx* in (from left to right) a control embryo, an embryo injected with εmor (3.5 ng), an embryo injected with *Gli-VP* (100 pg), and an embryo injected with *Gli-VP* and εmor. Embryos were bilaterally injected at the 8-cell stage.

pathway upstream of Gli remains intact in *B56ε* depleted embryos.

Above results demonstrate that *B56ε* is required for the Hh pathway. To address whether the defective eye field separation in εmor injected embryo is, indeed, caused by impaired Hh signaling, we asked whether Gli-VP could repress EFTF expression in the midline of εmor injected embryos. Thus, embryos were bilaterally injected with Gli-VP, εmor, or Gli-VP/εmor. Control and injected embryos were harvested at stage 20 and analyzed for *rx* expression.

Injection of *Gli-VP* RNA severely reduced *rx* expression, with 27% of embryo lacking *rx* expression completely and 73% of embryos exhibiting two faint *rx* expression domains ($n=44$). Consistent with previous results, 87% of εmor injected embryos exhibited a single *rx* expression domain ($n=33$). When Gli-VP was expressed in embryos injected with εmor, 73% of embryos exhibited two bilateral *rx* expression domains (although the level of *rx* expression was clearly reduced) and 27% of embryos lacked detectable *rx* expression ($n=48$) (Fig. 9F). Thus, Gli-VP was capable of suppressing EFTF expression in the midline of εmor injected embryos, indicating that the eye separation defect in *B56ε* depleted embryos is caused by impaired Hh signaling.

Discussion

Our results indicate that B56ε is a component shared by multiple signaling pathways. We have previously shown that B56ε is involved in the Wnt pathway (Yang et al., 2003). Wdb, the *Drosophila* homologue of B56ε, regulates the PCP pathway (Hannus et al., 2002). In this paper, we report that B56ε is required for the IGF/PI3K/Akt and the Hh pathways. Consistent with its roles in multiple signaling pathways, B56ε is expressed throughout the neural ectoderm (Yang et al., 2003) and regulates several processes during neural development. Depletion of *B56ε* in the neural ectoderm impairs the midbrain–hindbrain boundary formation, eye induction, eye field separation, and floor plate specific gene expression. It appears that different levels of B56ε are required for these developmental processes. Partial depletion of *B56ε* by injecting a lower dose of εmor blocks midbrain–hindbrain boundary formation, eye field separation, and floor plate specification, whereas eye induction defects occur only when the depletion of *B56ε* is more complete.

B56ε plays a direct role during eye induction

As a specialized extension of the anterior neural tissue, eye induction relies on proper axis specification, gastrulation, neural induction, forebrain induction, and regionalization within the forebrain. Any perturbation affecting these developmental processes will impair eye induction. Does B56ε regulate eye induction directly?

We have previously shown that depletion of maternal B56ε ventralizes embryos (Yang et al., 2003). When embryos were injected with εmor at the 8-cell stage, however, axis specification, neural induction, and forebrain specification occurred properly, as judged by the normal expression of dorsal ventral specific genes, a pan-neural marker, and a pan-forebrain marker. Similar to our results, it has been reported that injection of a dominant negative *frizzled7* or antisense oligos against *wnt11*, *FRL1*, or *X.EXT1* into oocytes, but not fertilized embryos, causes ventralization (Sumanas et al., 2000; Tao et al., 2005). This is likely because axis specification occurs shortly after fertilization. Interfering with Wnt signaling early during development, as opposed to later, ventralizes embryos (Darken and Wilson, 2001; Yang et al., 2002). As injection of εmor at the 8-cell stage does not ventralize embryos, eye development defects in B56ε depleted embryos were not caused by ventralization.

Injection of higher doses of εmor impairs blastopore closure. This phenotype is likely a consequence of the loss of B56ε, because embryos injected with the control morpholino had no gastrulation defects. While gastrulation defects certainly affect eye development to some degree, we found that the impaired eye development and the gastrulation defect observed in εmor injected embryos could be uncoupled. For example, when lower doses of εmor (2.5 ng–4.5 ng) was injected, or when εmor was injected at the 32-cell stage, embryos exhibited abnormal EFTFs expression and defective eye development without having gastrulation defect. These results demonstrate a direct role of B56ε in regulation of EFTFs expression and eye development.

Our data argues that depletion of *B56ε* does not block the eye field specification per se. Depletion of *B56ε* had differential effects on individual EFTFs during the eye induction phase. While injection of εmor severely blocked the initiation of *rx* and *lhx2,* the expression of *six3*, *pax6* and *ET* were only moderately reduced. These observations demonstrate that the eye field specification occurred in *B56ε* depleted embryos. In agreement with this interpretation, we failed to detect any expansion of posterior markers, despite observing a reduction in some of the regional brain markers (*arx*, *emoesodermin*, and *pax2*), suggesting a yet unknown role of B56ε in brain patterning. As development proceeds, the eye defects became more severe. Embryos substantially lost *six3* expression, which was only slightly reduced during earlier stages. Given that EFTFs regulate each other (Bailey et al., 2004; Chow and Lang, 2001; Mathers and Jamrich, 2000; Zuber et al., 2003), it is likely that *B56ε* depleted embryos lost *six3* expression during later stages, because the expression of *rx* and *lhx2* was down-regulated. Taken together, our results indicate that B56ε is involved in the initiation of a subset of EFTFs during eye induction.

Signaling pathway(s) mediated by B56ε during eye induction

Several signaling pathways are involved in early eye development. These include the IGF pathway (Eivers et al., 2004; Pera et al., 2003; Pera et al., 2001; Richard-Parpaillon et al., 2002), the Wnt pathway (Cavodeassi et al., 2005; Esteve et al., 2004; Maurus et al., 2005; Rasmussen et al., 2001; Van Raay et al., 2005), and the PCP pathway (Cavodeassi et al., 2005; Lee et al., 2006; Moore et al., 2004). Among these, IGF1 is a potent neural and forebrain inducer and induces EFTFs expression efficiently in *Xenopus* and *Zebrafish* embryos

(Eivers et al., 2004; Pera et al., 2003; Pera et al., 2001; Richard-Parpaillon et al., 2002). IGF activates both the MAPK and the PI3K/Akt pathways in most experimental settings (Oldham and Hafen, 2003). In particular, IGF/MAPK signaling has been implicated in neural induction (Kuroda et al., 2005; Linker and Stern, 2004; Pera et al., 2003). It remains unclear how IGF downstream pathways regulate eye development.

We provide evidence that B56ε regulates PI3K/Akt signaling downstream of IGF. Depletion of *B56ε* blocked IGF1-induced Akt phosphorylation, but had no effect on MAPK phosphorylation. Moreover, P110*-induced Akt phosphorylation was not sensitive to *B56ε* depletion. This is consistent with a recent study, showing that B56 family members are required for Akt phosphorylation in PC12 cells (Van Kanegan et al., 2005), and suggests that B56ε is required for the PI3K/Akt pathway upstream of, or at the parallel level of, PI3K.

In addition, our data demonstrates that the PI3K/Akt pathway is essential for eye induction. In agreement with this view, ectopic EFTFs expression induced by IGF1 was blocked by Δp85 or dnAkt in whole embryos. In animal caps, IGF1-induced EFTFs expression was inhibited by LY294002, a PI3K inhibitor. Moreover, interfering with the PI3K/Akt pathway impaired endogenous EFTFs expression and blocked eye formation. Notably, in all these experimental settings, neural or forebrain markers (*sox3* and *otx2*) were expressed normally. Thus, while it appears that IGF/MAPK signaling functions in neural induction, the IGF/PI3K/Akt pathway (maybe together with other pathways) is involved in eye induction. Thus, for the first time, we show that the IGF/PI3K/Akt pathway is essential for eye induction. Further experiments are needed to better understand the detailed mechanism through which PI3K/Akt pathway regulates eye induction.

To our surprise, overexpression of ca-Akt or P110* did not significantly rescue *rx* expression in εmor injected embryos (not shown). This may indicate that B56ε mediates multiple eye induction signaling pathways. While overexpression of ca-Akt or P110* restores Akt signaling, other B56ε-dependent eye induction pathways may still be inhibited in *B56ε* depleted embryos. What may be other B56ε-dependent eye induction pathways? As a Dishevelled interacting protein (Ratcliffe et al., 2000), B56ε is required for the canonical Wnt pathway in *Xenopus* (Yang et al., 2003). Its homologue, Wdb, is involved in the PCP pathway in *Drosophila* and regulates convergent extension during *Zebrafish* development (Hannus et al., 2002). Both the Wnt and the PCP pathways are important for eye development. The canonical Wnt pathway seems to play dual roles during eye development. Wnt signaling promotes the proliferation of retina progenitor cells within the eye field and expands the retina progenitor cell lineage through *sox2* (Van Raay et al., 2005). Under certain conditions, activation of the canonical Wnt pathway induces ectopic eyes (Rasmussen et al., 2001), likely through stimulating retina progenitor cell proliferation. During eye induction, however, Wnt signaling caudalizes the forebrain and antagonizes eye field specification (Cavodeassi et al., 2005; Esteve et al., 2004). Therefore, it is unlikely that the B56ε-dependent canonical Wnt pathway activates the expression of EFTFs during eye induction. Interestingly, embryos injected with a higher dose of εmor, exhibited severe blastopore closure defects, a typical PCP related phenotype. This suggests that *Xenopus* B56ε, like its *Drosophila* homologue Wdb, may be involved in the PCP pathway as well. Contrary to the inhibitory effect of the canonical Wnt pathway on eye induction, the PCP pathway is required for eye induction. In *Zebrafish*, Wnt11 signaling antagonizes canonical Wnt signaling and promotes eye field specification within the forebrain. It also regulates morphogenesis within the nascent eye field (Cavodeassi et al., 2005). Similarly, the PCP pathway regulates eye field specification and the cell movement within the eye field in *Xenopus* (Lee et al., 2006; Maurus et al., 2005). Thus, it is possible that B56ε mediates both the PI3K/Akt and the PCP pathways during eye induction. Further experiments will be needed to determine whether B56ε is indeed a key player of the PCP pathway in Xenopus and whether B56ε regulates both the PI3K/Akt and the PCP pathways during eye induction.

B56ε mediates the Hh pathway during eye field separation

Depletion of *B56ε* impairs eye field separation. Our results indicate that the defective eye separation in *B56ε* depleted embryos is caused by the abnormal Hh signaling. We observed that εmor injected embryos not only developed cyclopic eyes, but also lost the expression of Hh target genes, including *shh*, *ptc-1*, *ptc-2*, and *foxA2*. In addition, *B56ε* depleted embryos could not respond to overexpressed Shh. The activities of Shh, Smo, and the wild-type Gli1 were B56ε-dependent, while constitutively active Gli1 (Gli-VP) bypassed the requirement of B56ε. This epistasis analysis suggests that B56ε regulates the Hh pathway at the level of Gli. In agreement with this interpretation, although *B56ε* depletion blocked Shh-induced target gene expression, the Hh pathway upstream of Gli appeared to remain intact in *B56ε* depleted embryos, as judged by results from Gli3 processing and Gli1/Cos2 complex dissociation assays. Importantly, when Hh signaling in *B56ε* depleted embryos was restored by overexpression of Gli-VP, the midline expression of *rx* was suppressed. Thus, B56ε mediates the Hh pathway during the eye field separation.

Interestingly, we found that depletion of *B56ε* has no effect on Gli1 nuclear translocation. In addition, the activity of a Gli1 mutant deficient for Sufu binding (Dunaeva et al., 2003) is still sensitive to *B56ε* depletion (data not shown). It will be of interest to test if B56ε regulates the DNA binding affinity of Gli protein or the interaction between Gli and transcriptional co-activators. PP2A has been implicated in the Hh pathway (Krishnan et al., 1997). As a regulatory subunit of PP2A, B56ε may regulate Gli phosphorylation. In *Drosophila*, Ci phosphorylation appears to be critical not only for Ci processing, but also for the formation or the function of Ci activator. The activity of an uncleavable Ci is still under the control of PKA (Wang et al., 1999). Similarly, Gli1, which does not undergo pathway regulated proteolytic processing, can be inhibited by PKA (Lee et al., 1997). While this work was in the final stage of preparation, Wdb, the *Drosophila* B56ε orthologue, was identified from a genome-wide screen for Hh pathway

components (Nybakken et al., 2005). Therefore, understanding how B56ε modulates the Hh pathway will likely uncover an important mechanism for Ci/Gli regulation.

Acknowledgments

This work was initiated when JY worked as a post-doc in Dr. Peter Klein's lab at Penn. We greatly appreciate Dr. Klein for supporting this work initially, sharing unpublished data and reagents, and providing valuable suggestions. We would like to thank Kenneth Ryan, William Harris, Tomas Pieler, Daniel Weinstein, Randy Moon, Jin-Kwan Han, Sudipto Roy, Ariel Ruiz i Altaba, Dan Kessler and Marcus Gustafsson for plasmids and reagents; Janet Heasman, Douglas Epstein, Jean-Pierre Saint-Jeannet, David Virshup, Stefan Strack, and Jinling Wu for helpful discussions; Peter Klein, Dan Kessler, John Barnard, and Jinling Wu for reading the manuscript. This work was supported by a CCRI internal startup grant to JY.

References

Alexandre, C., Jacinto, A., Ingham, P.W., 1996. Transcriptional activation of hedgehog target genes in *Drosophila* is mediated directly by the Cubitus interruptus protein, a member of the GLI family of zinc finger DNA-binding proteins. Genes Dev. 10, 2003–2013.

Ashery-Padan, R., Gruss, P., 2001. Pax6 lights-up the way for eye development. Curr. Opin. Cell Biol. 13, 706–714.

Aza-Blanc, P., Ramirez-Weber, F.A., Laget, M.P., Schwartz, C., Kornberg, T.B., 1997. Proteolysis that is inhibited by hedgehog targets Cubitus interruptus protein to the nucleus and converts it to a repressor. Cell 89, 1043–1053.

Bachy, I., Vernier, P., Retaux, S., 2001. The LIM-homeodomain gene family in the developing *Xenopus* brain: conservation and divergences with the mouse related to the evolution of the forebrain. J. Neurosci. 21, 7620–7629.

Bailey, T.J., El-Hodiri, H., Zhang, L., Shah, R., Mathers, P.H., Jamrich, M., 2004. Regulation of vertebrate eye development by *Rx* genes. Int. J. Dev. Biol. 48, 761–770.

Bouwmeester, T., Kim, S., Sasai, Y., Lu, B., De Robertis, E.M., 1996. Cerberus is a head-inducing secreted factor expressed in the anterior endoderm of Spemann's organizer. Nature 382, 595–601.

Carballada, R., Yasuo, H., Lemaire, P., 2001. Phosphatidylinositol-3 kinase acts in parallel to the ERK MAP kinase in the FGF pathway during *Xenopus* mesoderm induction. Development 128, 35–44.

Cavodeassi, F., Carreira-Barbosa, F., Young, R.M., Concha, M.L., Allende, M.L., Houart, C., Tada, M., Wilson, S.W., 2005. Early stages of zebrafish eye formation require the coordinated activity of Wnt11, Fz5, and the Wnt/beta-catenin pathway. Neuron 47, 43–56.

Chiang, C., Litingtung, Y., Lee, E., Young, K.E., Corden, J.L., Westphal, H., Beachy, P.A., 1996. Cyclopia and defective axial patterning in mice lacking Sonic hedgehog gene function. Nature 383, 407–413.

Cho, K.W., Blumberg, B., Steinbeisser, H., De Robertis, E.M., 1991. Molecular nature of Spemann's organizer: the role of the *Xenopus* homeobox gene goosecoid. Cell 67, 1111–1120.

Chow, R.L., Lang, R.A., 2001. Early eye development in vertebrates. Annu. Rev. Cell Dev. Biol. 17, 255–296.

Darken, R.S., Wilson, P.A., 2001. Axis induction by wnt signaling: target promoter responsiveness regulates competence. Dev. Biol. 234, 42–54.

De Robertis, E.M., Kuroda, H., 2004. Dorsal–ventral patterning and neural induction in *Xenopus* embryos. Annu. Rev. Cell Dev. Biol. 20, 285–308.

Dunaeva, M., Michelson, P., Kogerman, P., Toftgard, R., 2003. Characterization of the physical interaction of Gli proteins with SUFU proteins. J. Biol. Chem. 278, 5116–5122.

Eivers, E., McCarthy, K., Glynn, C., Nolan, C.M., Byrnes, L., 2004. Insulin-like growth factor (IGF) signalling is required for early dorso-anterior development of the zebrafish embryo. Int. J. Dev. Biol. 48, 1131–1140.

Ekker, S.C., McGrew, L.L., Lai, C.J., Lee, J.J., von Kessler, D.P., Moon, R.T., Beachy, P.A., 1995. Distinct expression and shared activities of members of the hedgehog gene family of *Xenopus laevis*. Development 121, 2337–2347.

Esteve, P., Lopez-Rios, J., Bovolenta, P., 2004. SFRP1 is required for the proper establishment of the eye field in the medaka fish. Mech. Dev. 121, 687–701.

Gao, Z.H., Seeling, J.M., Hill, V., Yochum, A., Virshup, D.M., 2002. Casein kinase I phosphorylates and destabilizes the beta-catenin degradation complex. Proc. Natl. Acad Sci. U. S. A. 99, 1182–1187.

Glinka, A., Wu, W., Delius, H., Monaghan, A.P., Blumenstock, C., Niehrs, C., 1998. Dickkopf-1 is a member of a new family of secreted proteins and functions in head induction. Nature 391, 357–362.

Hammerschmidt, M., Pelegri, F., Mullins, M.C., Kane, D.A., Brand, M., van Eeden, F.J., Furutani-Seiki, M., Granato, M., Haffter, P., Heisenberg, C.P., Jiang, Y.J., Kelsh, R.N., Odenthal, J., Warga, R.M., Nusslein-Volhard, C., 1996. Mutations affecting morphogenesis during gastrulation and tail formation in the zebrafish, *Danio rerio*. Development 123, 143–151.

Hammerschmidt, M., Brook, A., McMahon, A.P., 1997. The world according to hedgehog. Trends Genet. 13, 14–121.

Hannus, M., Feiguin, F., Heisenberg, C.P., Eaton, S., 2002. Planar cell polarization requires Widerborst, a B′ regulatory subunit of protein phosphatase 2A. Development 129, 3493–3503.

Harland, R., Gerhart, J., 1997. Formation and function of Spemann's organizer. Annu. Rev. Cell Dev. Biol. 13, 611–667.

Heasman, J., 1997. Patterning the *Xenopus* blastula. Development 124, 4179–4191.

Heisenberg, C.P., Nusslein-Volhard, C., 1997. The function of silberblick in the positioning of the eye anlage in the zebrafish embryo. Dev. Biol. 184, 85–94.

Heisenberg, C.P., Brand, M., Jiang, Y.J., Warga, R.M., Beuchle, D., van Eeden, F.J., Furutani-Seiki, M., Granato, M., Haffter, P., Hammerschmidt, M., Kane, D.A., Kelsh, R.N., Mullins, M.C., Odenthal, J., Nusslein-Volhard, C., 1996. Genes involved in forebrain development in the zebrafish, *Danio rerio*. Development 123, 191–203.

Heller, N., Brandli, A.W., 1997. *Xenopus* Pax-2 displays multiple splice forms during embryogenesis and pronephric kidney development. Mech. Dev. 69, 83–104.

Huangfu, D., Anderson, K.V., 2006. Signaling from *Smo* to *Ci/Gli*: conservation and divergence of Hedgehog pathways from *Drosophila* to vertebrates. Development 133, 3–14.

Ingham, P.W., McMahon, A.P., 2001. Hedgehog signaling in animal development: paradigms and principles. Genes Dev. 15, 3059–3087.

James, J., Das, A.V., Rahnenfuhrer, J., Ahmad, I., 2004. Cellular and molecular characterization of early and late retinal stem cells/progenitors: differential regulation of proliferation and context dependent role of Notch signaling. J. Neurobiol. 61, 359–376.

Janssens, V., Goris, J., 2001. Protein phosphatase 2A: a highly regulated family of serine/threonine phosphatases implicated in cell growth and signalling. Biochem. J. 353, 417–439.

Kao, K.R., Elinson, R.P., 1988. The entire mesodermal mantle behaves as Spemann's organizer in dorsoanterior enhanced *Xenopus laevis* embryos. Dev. Biol. 127, 64–77.

Keeler, R.F., 1970. Teratogenic compounds of *Veratrum californicum* (Durand): X. Cyclopia in rabbits produced by cyclopamine. Teratology 3, 175–180.

Koebernick, K., Hollemann, T., Pieler, T., 2001. Molecular cloning and expression analysis of the Hedgehog receptors XPtc1 and XSmo in *Xenopus laevis*. Mech. Dev. 100, 303–308.

Koebernick, K., Hollemann, T., Pieler, T., 2003. A restrictive role for Hedgehog signalling during otic specification in *Xenopus*. Dev. Biol. 260, 325–338.

Krishnan, V., Pereira, F.A., Qiu, Y., Chen, C.H., Beachy, P.A., Tsai, S.Y., Tsai, M.J., 1997. Mediation of Sonic hedgehog-induced expression of COUP-TFII by a protein phosphatase. Science 278, 1947–1950.

Kuroda, H., Fuentealba, L., Ikeda, A., Reversade, B., De Robertis, E.M., 2005. Default neural induction: neuralization of dissociated *Xenopus* cells is mediated by Ras/MAPK activation. Genes Dev. 19, 1022–1027.

Lee, J., Platt, K.A., Censullo, P., Ruizi Altaba, A., 1997. Gli1 is a target of Sonic hedgehog that induces ventral neural tube development. Development 124, 2537–2552.

Lee, H.S., Bong, Y.S., Moore, K.B., Soria, K., Moody, S.A., Daar, I.O., 2006. Dishevelled mediates ephrinB1 signalling in the eye field through the planar cell polarity pathway. Nat. Cell Biol. 8, 55–63.

Li, H., Tierney, C., Wen, L., Wu, J.Y., Rao, Y., 1997. A single morphogenetic field gives rise to two retina primordia under the influence of the prechordal plate. Development 124, 603–615.

Li, X., Yost, H.J., Virshup, D.M., Seeling, J.M., 2001. Protein phosphatase 2A and its B56 regulatory subunit inhibit Wnt signaling in *Xenopus*. EMBO J. 20, 4122–4131.

Li, X., Scuderi, A., Letsou, A., Virshup, D.M., 2002. B56-associated protein phosphatase 2A is required for survival and protects from apoptosis in *Drosophila melanogaster*. Mol. Cell. Biol. 22, 3674–3684.

Linker, C., Stern, C.D., 2004. Neural induction requires BMP inhibition only as a late step, and involves signals other than FGF and Wnt antagonists. Development 131, 5671–5681.

Ma, Y., Erkner, A., Gong, R., Yao, S., Taipale, J., Basler, K., Beachy, P.A., 2002. Hedgehog-mediated patterning of the mammalian embryo requires transporter-like function of dispatched. Cell 111, 63–75.

Marlow, F., Zwartkruis, F., Malicki, J., Neuhauss, S.C., Abbas, L., Weaver, M., Driever, W., Solnica-Krezel, L., 1998. Functional interactions of genes mediating convergent extension, knypek and trilobite, during the partitioning of the eye primordium in zebrafish. Dev. Biol. 203, 382–399.

Marti, E., Takada, R., Bumcrot, D.A., Sasaki, H., McMahon, A.P., 1995. Distribution of Sonic hedgehog peptides in the developing chick and mouse embryo. Development 121, 2537–2547.

Mathers, P.H., Jamrich, M., 2000. Regulation of eye formation by the *Rx* and *pax6* homeobox genes. Cell. Mol. Life Sci. 57, 186–194.

Mathers, P.H., Grinberg, A., Mahon, K.A., Jamrich, M., 1997. The *Rx* homeobox gene is essential for vertebrate eye development. Nature 387, 603–607.

Maurus, D., Heligon, C., Burger-Schwarzler, A., Brandli, A.W., Kuhl, M., 2005. Noncanonical Wnt-4 signaling and EAF2 are required for eye development in *Xenopus laevis*. EMBO J. 24, 1181–1191.

McCright, B., Virshup, D.M., 1995. Identification of a new family of protein phosphatase 2A regulatory subunits. J. Biol. Chem. 270, 26123–26128.

McMahon, A.P., Ingham, P.W., Tabin, C.J., 2003. Developmental roles and clinical significance of hedgehog signaling. Curr. Top. Dev. Biol. 53, 1–114.

Moody, S.A., 1987a. Fates of the blastomeres of the 16-cell stage *Xenopus* embryo. Dev. Biol. 119, 560–578.

Moody, S.A., 1987b. Fates of the blastomeres of the 32-cell-stage *Xenopus* embryo. Dev. Biol. 122, 300–319.

Moore, K.B., Mood, K., Daar, I.O., Moody, S.A., 2004. Morphogenetic movements underlying eye field formation require interactions between the FGF and ephrinB1 signaling pathways. Dev. Cell 6, 55–67.

Nybakken, K., Vokes, S.A., Lin, T.Y., McMahon, A.P., Perrimon, N., 2005. A genome-wide RNA interference screen in *Drosophila melanogaster* cells for new components of the Hh signaling pathway. Nat. Genet. 37, 1323–1332.

Oldham, S., Hafen, E., 2003. Insulin/IGF and target of rapamycin signaling: a TOR de force in growth control. Trends Cell Biol. 13, 79–85.

Oliver, G., Mailhos, A., Wehr, R., Copeland, N.G., Jenkins, N.A., Gruss, P., 1995. *Six3*, a murine homologue of the sine oculis gene, demarcates the most anterior border of the developing neural plate and is expressed during eye development. Development 121, 4045–4055.

Pannese, M., Polo, C., Andreazzoli, M., Vignali, R., Kablar, B., Barsacchi, G., Boncinelli, E., 1995. The *Xenopus* homologue of *Otx2* is a maternal homeobox gene that demarcates and specifies anterior body regions. Development 121, 707–720.

Penzel, R., Oschwald, R., Chen, Y., Tacke, L., Grunz, H., 1997. Characterization and early embryonic expression of a neural specific transcription factor xSOX3 in *Xenopus laevis*. Int. J. Dev. Biol. 41, 667–677.

Pera, E.M., Wessely, O., Li, S.Y., De Robertis, E.M., 2001. Neural and head induction by insulin-like growth factor signals. Dev. Cell 1, 655–665.

Pera, E.M., Ikeda, A., Eivers, E., De Robertis, E.M., 2003. Integration of IGF, FGF, and anti-BMP signals via Smad1 phosphorylation in neural induction. Genes Dev. 17, 3023–3028.

Rasmussen, J.T., Deardorff, M.A., Tan, C., Rao, M.S., Klein, P.S., Vetter, M.L., 2001. Regulation of eye development by frizzled signaling in *Xenopus*. Proc. Natl. Acad Sci. U. S. A. 98, 3861–3866.

Ratcliffe, M.J., Itoh, K., Sokol, S.Y., 2000. A positive role for the PP2A catalytic subunit in Wnt signal transduction. J. Biol. Chem. 275, 35680–35683.

Rembold, M., Loosli, F., Adams, R.J., Wittbrodt, J., 2006. Individual cell migration serves as the driving force for optic vesicle evagination. Science 313, 1130–1134.

Richard-Parpaillon, L., Heligon, C., Chesnel, F., Boujard, D., Philpott, A., 2002. The IGF pathway regulates head formation by inhibiting Wnt signaling in *Xenopus*. Dev. Biol. 244, 407–417.

Roessler, E., Belloni, E., Gaudenz, K., Jay, P., Berta, P., Scherer, S.W., Tsui, L.C., Muenke, M., 1996. Mutations in the human Sonic Hedgehog gene cause holoprosencephaly. Nat. Genet. 14, 357–360.

Ruiz i Altaba, A., 1999. Gli proteins encode context-dependent positive and negative functions: implications for development and disease. Development 126, 3205–3216.

Ruiz i Altaba, A., Prezioso, V.R., Darnell, J.E., Jessell, T.M., 1993. Sequential expression of HNF-3 beta and HNF-3 alpha by embryonic organizing centers: the dorsal lip/node, notochord and floor plate. Mech. Dev. 44, 91–108.

Ryan, K., Butler, K., Bellefroid, E., Gurdon, J.B., 1998. *Xenopus* eomesodermin is expressed in neural differentiation. Mech. Dev. 75, 155–158.

Salic, A.N., Kroll, K.L., Evans, L.M., Kirschner, M.W., 1997. Sizzled: a secreted Xwnt8 antagonist expressed in the ventral marginal zone of *Xenopus* embryos. Development 124, 4739–4748.

Salzberg, A., Elias, S., Nachaliel, N., Bonstein, L., Henig, C., Frank, D., 1999. A Meis family protein caudalizes neural cell fates in *Xenopus*. Mech. Dev. 80, 3–13.

Sasai, Y., Lu, B., Steinbeisser, H., Geissert, D., Gont, L.K., De Robertis, E.M., 1994. *Xenopus* chordin: a novel dorsalizing factor activated by organizer-specific homeobox genes. Cell 79, 779–790.

Seeling, J.M., Miller, J.R., Gil, R., Moon, R.T., White, R., Virshup, D.M., 1999. Regulation of beta-catenin signaling by the B56 subunit of protein phosphatase 2A. Science 283, 2089–2091.

Seufert, D.W., Prescott, N.L., El-Hodiri, H.M., 2005. *Xenopus aristaless*-related homeobox (*xARX*) gene product functions as both a transcriptional activator and repressor in forebrain development. Dev. Dyn. 232, 313–324.

Shimamura, K., Hartigan, D.J., Martinez, S., Puelles, L., Rubenstein, J.L., 1995. Longitudinal organization of the anterior neural plate and neural tube. Development 121, 3923–3933.

Silverstein, A.M., Barrow, C.A., Davis, A.J., Mumby, M.C., 2002. Actions of PP2A on the MAP kinase pathway and apoptosis are mediated by distinct regulatory subunits. Proc. Natl. Acad Sci. U. S. A. 99, 4221–4226.

Sive, H., Grainger, R., Harland, R., 2000. Early Development of *Xenopus laevis*; A Laboratory Manual. Cold Spring Harbor Press, Cold Spring Harbor.

Smith, W.C., McKendry, R., Ribisi, S., Harland, R.M., 1995. A nodal-related gene defines a physical and functional domain within the Spemann organizer. Cell 82, 37–46.

Solnica-Krezel, L., Stemple, D.L., Mountcastle-Shah, E., Rangini, Z., Neuhauss, S.C., Malicki, J., Schier, A.F., Stainier, D.Y., Zwartkruis, F., Abdelilah, S., Driever, W., 1996. Mutations affecting cell fates and cellular rearrangements during gastrulation in zebrafish. Development 123, 67–80.

Stern, C.D., 2005. Neural induction: old problem, new findings, yet more questions. Development 132, 2007–2021.

Stoykova, A., Fritsch, R., Walther, C., Gruss, P., 1996. Forebrain patterning defects in small eye mutant mice. Development 122, 3453–3465.

Sumanas, S., Strege, P., Heasman, J., Ekker, S.C., 2000. The putative wnt receptor *Xenopus* frizzled-7 functions upstream of beta-catenin in vertebrate dorsoventral mesoderm patterning. Development 127, 1981–1990.

Suri, C., Haremaki, T., Weinstein, D.C., 2004. Inhibition of mesodermal fate by *Xenopus* HNF3beta/FoxA2. Dev. Biol. 265, 90–104.

Takabatake, T., Takahashi, T.C., Takabatake, Y., Yamada, K., Ogawa, M., Takeshima, K., 2000. Distinct expression of two types of *Xenopus* patched genes during early embryogenesis and hindlimb development. Mech. Dev. 98, 99–104.

Tao, Q., Yokota, C., Puck, H., Kofron, M., Birsoy, B., Yan, D., Asashima, M., Wylie, C.C., Lin, X., Heasman, J., 2005. Maternal wnt11 activates the canonical wnt signaling pathway required for axis formation in *Xenopus* embryos. Cell 120, 857–871.

Tay, S.Y., Ingham, P.W., Roy, S., 2005. A homologue of the *Drosophila* kinesin-like protein Costal2 regulates Hedgehog signal transduction in the vertebrate embryo. Development 132, 625–634.

Van Kanegan, M.J., Adams, D.G., Wadzinski, B.E., Strack, S., 2005. Distinct protein phosphatase 2A heterotrimers modulate growth factor signaling to extracellular signal-regulated kinases and Akt. J. Biol. Chem. 280, 36029–36036.

Van Raay, T.J., Moore, K.B., Iordanova, I., Steele, M., Jamrich, M., Harris, W.A., Vetter, M.L., 2005. Frizzled 5 signaling governs the neural potential of progenitors in the developing *Xenopus* retina. Neuron 46, 23–36.

Wallis, D., Muenke, M., 2000. Mutations in holoprosencephaly. Hum. Mutat. 16, 99–108.

Wang, G., Wang, B., Jiang, J., 1999. Protein kinase A antagonizes Hedgehog signaling by regulating both the activator and repressor forms of Cubitus interruptus. Genes Dev. 13, 2828–2837.

Wang, B., Fallon, J.F., Beachy, P.A., 2000. Hedgehog-regulated processing of Gli3 produces an anterior/posterior repressor gradient in the developing vertebrate limb. Cell 100, 423–434.

Woo, K., Fraser, S.E., 1995. Order and coherence in the fate map of the zebrafish nervous system. Development 121, 2595–2609.

Woo, K., Shih, J., Fraser, S.E., 1995. Fate maps of the zebrafish embryo. Curr. Opin. Genet. Dev. 5, 439–443.

Wu, J., O'Donnell, M., Gitler, A.D., Klein, P.S., 2006. Kermit 2/XGIPC, an IGF1 receptor interacting protein, is required for IGF signaling in *Xenopus* eye development. Development 133, 3651–3660.

Xanthos, J.B., Kofron, M., Tao, Q., Schaible, K., Wylie, C., Heasman, J., 2002. The roles of three signaling pathways in the formation and function of the Spemann organizer. Development 129, 4027–4043.

Yang, J., Tan, C., Darken, R.S., Wilson, P.A., Klein, P.S., 2002. Beta-catenin/Tcf-regulated transcription prior to the midblastula transition. Development 129, 5743–5752.

Yang, J., Wu, J., Tan, C., Klein, P.S., 2003. PP2A:B56epsilon is required for Wnt/beta-catenin signaling during embryonic development. Development 130, 5569–5578.

Zhang, L., Mathers, P.H., Jamrich, M., 2000. Function of *Rx*, but not *Pax6*, is essential for the formation of retinal progenitor cells in mice. Genesis 28, 135–142.

Zhang, X.M., Ramalho-Santos, M., McMahon, A.P., 2001. Smoothened mutants reveal redundant roles for Shh and Ihh signaling including regulation of L/R symmetry by the mouse node. Cell 106, 781–792.

Zhang, W., Zhao, Y., Tong, C., Wang, G., Wang, B., Jia, J., Jiang, J., 2005. Hedgehog-regulated Costal2–kinase complexes control phosphorylation and proteolytic processing of Cubitus interruptus. Dev. Cell 8, 267–278.

Zhou, X., Hollemann, T., Pieler, T., Gruss, P., 2000. Cloning and expression of xSix3, the *Xenopus* homologue of murine Six3. Mech. Dev. 91, 327–330.

Zuber, M.E., Perron, M., Philpott, A., Bang, A., Harris, W.A., 1999. Giant eyes in *Xenopus laevis* by overexpression of XOptx2. Cell 98, 341–352.

Zuber, M.E., Gestri, G., Viczian, A.S., Barsacchi, G., Harris, W.A., 2003. Specification of the vertebrate eye by a network of eye field transcription factors. Development 130, 5155–5167.